NASA TECHNICAL NOTE

NASA TN D-7088

NASA TN D-7088

LEE-SURFACE HEATING AND FLOW PHENOMENA ON SPACE SHUTTLE ORBITERS AT LARGE ANGLES OF ATTACK AND HYPERSONIC SPEEDS

by Jerry N. Hefner

Langley Research Center
Hampton, Va. 23365

NATIONAL AERONAUTICS AND SPACE ADMINISTRATION • WASHINGTON, D. C. • NOVEMBER 1972

1. Report No.	2. Government Accession No.	3. Recipient's Catalog No.
NASA TN D-7088		

4. Title and Subtitle	5. Report Date
LEE-SURFACE HEATING AND FLOW PHENOMENA ON SPACE SHUTTLE ORBITERS AT LARGE ANGLES OF ATTACK AND HYPERSONIC SPEEDS	November 1972
	6. Performing Organization Code
7. Author(s)	8. Performing Organization Report No.
Jerry N. Hefner	L-8580
9. Performing Organization Name and Address	10. Work Unit No.
NASA Langley Research Center Hampton, Va. 23365	502-37-01-11
	11. Contract or Grant No.
12. Sponsoring Agency Name and Address	13. Type of Report and Period Covered
National Aeronautics and Space Administration Washington, D.C. 20546	Technical Note
	14. Sponsoring Agency Code

15. Supplementary Notes

16. Abstract

The lee-surface flow phenomena on a delta-wing orbiter and a straight-wing orbiter have been investigated at angles of attack between 0^{o} and 50^{o} at a Mach number of 6. Limited studies of the delta-wing orbiter were conducted at a Mach number of 19. Heat-transfer data, pressure distributions, and oil-flow studies were employed to experimentally examine the nature of the surface flow and the severity of the lee-surface heating. The effects of Reynolds number on the flow field and heating were investigated. Problem areas are defined and areas for further study are recommended.

17. Key Words (Suggested by Author(s))	18. Distribution Statement
Heat transfer Lee side Shuttle	Unclassified – Unlimited

19. Security Classif. (of this report)	20. Security Classif. (of this page)	21. No. of Pages	22. Price*
Unclassified	Unclassified	42	$3.00

*For sale by the National Technical Information Service, Springfield, Virginia 22151

LEE-SURFACE HEATING AND FLOW PHENOMENA ON SPACE SHUTTLE ORBITERS AT LARGE ANGLES OF ATTACK AND HYPERSONIC SPEEDS

By Jerry N. Hefner
Langley Research Center

SUMMARY

The lee-surface flow phenomena on a delta-wing orbiter and a straight-wing orbiter at angles of attack between 0° and 50° have been investigated at a free-stream Mach number of 6. Limited studies of the delta-wing orbiter were conducted at a Mach number of 19. Heat-transfer data, pressure distributions, and oil-flow studies were employed to experimentally examine the nature of the surface flow and the severity of the lee-surface heating. Reynolds number and angle of attack were found to significantly affect the severe vortex-induced peak heating on the lee surfaces of the orbiters. Vortex-induced heating was found to be extremely geometry dependent, and modifications to the lee-surface geometry reduced the severity of the lee-surface heating. Problem areas are defined and areas for further study are recommended.

INTRODUCTION

Lee-surface heating on space-shuttle configurations has often been regarded as relatively insignificant since the lee surfaces are generally sheltered from the main stream. However, recent experimental studies have shown the strong influence of vortices on the lee-surface heating on several conceptual shuttle orbiters. (See refs. 1 to 5.) The present report discusses and summarizes the results of an experimental program to evaluate the lee-surface heating and flow field on space-shuttle-type geometries. Some of the results of this program have been reported by the present author in references 1 and 2.

The present investigation of the lee-surface flow phenomena was conducted on a delta-wing orbiter and a straight-wing orbiter at a free-stream Mach number of 6. Limited studies of the delta-wing orbiter were also conducted at a Mach number of 19. Heat-transfer data obtained by the phase-change-paint technique (ref. 6), pressure distributions, and oil-flow studies were employed to experimentally examine the nature of the surface flow and the severity of the lee-surface heating. Variables in the investigation included free-stream Reynolds number (0.36×10^7 to 2.52×10^7 per meter), angle of attack (0°

to 50°), and modifications to nose and lee-surface geometry. Problem areas are defined and areas for further study are recommended.

SYMBOLS

h	local heat-transfer coefficient
h_{ref}	stagnation heat-transfer coefficient on a 0.305-m-radius sphere scaled by same factor as wind-tunnel model
L	model length
M_∞	free-stream Mach number
$N_{St,\infty}$	free-stream Stanton number
p	static pressure
R_∞	free-stream unit Reynolds number
$R_{\infty,L}$	free-stream Reynolds number based on model length
$R_{\infty,x}$	free-stream Reynolds number based on distance to peak heating
r	planform nose radius
T_w	radiation equilibrium surface temperature
x	longitudinal distance measured along surface from model nose
y	spanwise distance measured along surface from lee-surface meridian
α	angle of attack

Subscripts:

peak	conditions at position of maximum lee-surface vortex-induced heating
∞	free-stream conditions

APPARATUS AND METHODS

Tunnels

The studies at a Mach number of 6 were conducted in the Langley 20-inch Mach 6 tunnel. A complete description of this tunnel and its calibration is given in the appendix of reference 7.

The studies at a Mach number of 19 were conducted in the Langley hypersonic nitrogen tunnel. A description of this facility and its calibration is given in reference 8.

Model Description and Instrumentation

Two conceptual space shuttle orbiters were employed in the investigation and are shown in figure 1. The delta-wing orbiter (described in ref. 9) is representative of a high-cross-range configuration, and two scale models of it were tested – a 0.00635-scale model with $r/L = 0.02$ and a 0.00397-scale model with $r/L = 0.01$. The straight-wing orbiter (described in ref. 10) was selected to illustrate a gross difference in geometry and is representative of a low-cross-range orbiter. The scale of the straight-wing orbiter was 0.00725. Since the delta-wing orbiter is of much greater interest, the major emphasis of this paper will be placed on the delta-wing configuration.

Heat-transfer models used in the investigation were made of a mica-stycast resin. These models, together with additional aluminum models (0.00635-scale delta-wing orbiter and 0.00725-scale straight-wing orbiter), were used in the oil-flow studies. An aluminum 0.00635-scale delta-wing model was also instrumented with nine pressure orifices located along the lee-surface meridian.

Test Conditions

The tests at a Mach number of 6 were conducted at free-stream Reynolds numbers from 0.36×10^7 to 2.52×10^7 per meter. The total temperature was nearly constant at 497 K, and the wall-to-total temperature ratio was approximately 0.6. The angle of attack was varied from 0° to 50°.

The tests at a Mach number of 19 were conducted at a free-stream Reynolds number of 0.38×10^7 per meter. The total temperature was 1600 K, and the wall-to-total temperature ratio was approximately 0.2. Three angles of attack (0°, 20°, 37°) were examined.

Test Methods

Heat-transfer data were obtained by using the phase-change-paint technique (ref. 6) and were recorded on 35-mm motion-picture film at the rate of 10 frames per second.

The characteristics of the grid network used in determining the location of the constant-heating lines are shown in figure 2. Phase-change paints were utilized which allowed adequate data reduction with minimum conduction errors. Pressure data on the delta-wing orbiter were measured by multirange capacitance-type pressure transducers which were accurate to within 0.25 percent full scale, and the electrical output from these transducers was recorded on magnetic tape and processed by an electronic data processing system.

Oil-flow studies were conducted to examine the surface flow, relative shear, and separation boundaries on the upper surfaces of the orbiter body and wings. A mixture of silicon oil and lampblack was distributed in random dots of varying sizes over the entire upper surface of the model. Photographs were then taken of the models after each test.

Data Reduction

The heat-transfer data were reduced to local heat-transfer coefficients by the method of reference 6. Since recovery factors for lee-side flow are unknown, the present data are reduced assuming a laminar recovery factor of 0.86 based on free-stream conditions. The local heat-transfer coefficient was normalized by the calculated stagnation heat-transfer coefficient (method of Fay and Riddell, ref. 11) on a sphere having a 0.305-m radius scaled by the same factor as the model at the same test conditions. The local static pressure was normalized by the calculated free-stream static pressure based on the measured free-stream total pressure and Mach 6 flow.

RESULTS AND DISCUSSION

Flow-Field Characteristics

Oil-flow studies at Mach 6 on the upper surfaces of the delta-wing orbiter at angle of attack show the presence of numerous vortices and relatively large areas of flow separation with low shear. (See figs. 3 and 4.) The oil-flow photograph and schematic shown in figure 3 identify the various characteristics of the lee-surface flow. The schematic was developed by analyzing the results of the oil-flow studies by using knowledge of vortex flows over simplified geometries. The windward-surface flow expands around to the lee surface and remains attached for a finite distance before it separates and forms a vortex. Over the forward portion of the fuselage, this vortex scrubs the lee surface in the vicinity of the lee meridian (scrubbing action of vortices is indicated by featherlike oil smears) and induces a secondary vortex (smaller in size) as indicated in the schematic of figure 3. Over the aft portion of the fuselage, the windward-surface flow again expands around the wing leading edge and separates after remaining attached for a finite

distance. The vortex then interacts with the side of the fuselage. The outer streamlines of the viscous layer flow over the vortex and attach onto the lee surface, remain attached briefly, and then separate. This process gives rise to another vortex which lifts off the surface. A comparison of the heating distributions and oil-flow patterns in figure 4 shows that relatively high heating accompanies the interaction of the vortex with the lee surface, whereas lower heating accompanies separation and low surface shear.

Effect of Angle of Attack

Vortices strongly influence the surface flow and the heating on the delta-wing orbiter over the angle-of-attack range of 20° to 50°, with peak lee-surface heating occurring on the lee meridian, generally within the foremost 30 percent of the overall fuselage length. (See fig. 4.) Heating along the lee-surface meridian is presented in figure 5 for various angles of attack. Several heating peaks (all of which exceed the heating at zero angle of attack) are generated as the angle of attack is increased. The first of these peaks is always the maximum and occurs within a region where vortices, shed from the foremost portion of the fuselage, interact with the surface. (Compare the oil flow and heating in fig. 4.) An explanation of how the other heating peaks originate is not available at this time, and basic fluid-mechanic studies are needed to provide an understanding of these phenomena. However, with the aid of the oil-flow photographs in figure 4, one could postulate that after the initial vortex-surface interaction a boundary-layer-type flow is reestablished on the lee surface. This flow is subject to numerous influences such as transition, separation, and varying cross flow. Nevertheless, the maximum lee-meridian heating increases rapidly as the angle of attack approaches 30° (fig. 6(a)) and tends to level off between angles of attack of 30° and 45°. Increasing angle of attack has a significant effect on the position of peak heating, especially to 35° angle of attack. (See fig. 6(b).)

The heating along the lee meridian does not vary in proportion with the lee-meridan pressures. (See fig. 7.) The surface pressures show no abrupt increases in the regions of peak heating. In fact, the magnitude of the pressures at the position of peak heating is nearly constant with increasing angle of attack. This result is in contrast to the heating behavior with angle of attack and indicates that the peak heating is not caused by simply an abrupt increase in static pressure. A more probable explanation is that the peak heating is caused by the thinning of the viscous shear layer (which acts as an insulator against the high-energy inviscid flow) as a result of outflow induced by the vortices. A similar explanation was given in reference 12 for vortex-induced heating on a planar delta wing at low incidence. Limited vapor-screen tests were conducted on the lee surface of the delta-wing orbiter to evaluate this concept; however, details of the flow field were obscured apparently by the large entropy gradients generated by the windward surface and blunt nose (fig. 8).

The severity of the peak heating on the delta-wing orbiter is evident when the heating rates are converted to radiation equilibrium temperatures (fig. 5) and these temperatures are compared with the structural limits for titanium (approximately 620 K). The resulting temperatures varied from 455 K to a peak of 670 K for an angle of attack of 20° assuming an emissivity of 0.8 and a maximum stagnation heat-transfer rate for a typical 1500-nautical-mile cross-range trajectory (ref. 13) of 136 kW/m^2. (See fig. 5.) This result is dependent upon the choice of the trajectory used in the calculation procedure.

Lee-surface heating exceeding that at zero angle of attack is not confined to the region of the meridian since vortices also interact with the sides of the orbiter fuselage. (See oil-flow photographs in fig. 4.) Spanwise heating at several longitudinal locations are shown in figure 9 for angles of attack of 0°, 20°, and 40°. The composite sketch in figure 10 illustrates graphically the regions of heating above that at zero angle of attack.

As evidenced by figures 3 to 10, it is important to realize that heating data generated for only selected longitudinal locations on a given geometry do not define the lee-surface flow phenomena since the heating is nonuniform. This is particularly true when data sufficiently close to the nose have not been obtained.

Effect of Reynolds Number

The present results show that Reynolds number strongly influences the lee-surface heating. On the lee meridian of the delta-wing orbiter models, increasing Reynolds number increases vortex-induced peak heating over the forward portion of the fuselage ($x/L < 0.5$) and decreases the heating in the separated flow region over the aft portion of the fuselage. (See figs. 11 and 12.) Static pressures (fig. 13) along the lee meridian decreased with increasing Reynolds number. This behavior in the separated flow region over the aft portion of the fuselage is indicative of transitional base flow separation (ref. 14) and helps to explain the decrease in heating in that area.

Although the heating distributions for the two different scale orbiter models differ slightly, the heating peaks over the forward portion of both models evolve progressively with increasing Reynolds number. (See figs. 11 and 12.) Note the absence of peak heating for $x/L < 0.5$ on the smaller scale orbiter at $\alpha = 20^{\circ}$ for body-length Reynolds numbers of 1.2×10^6 and 0.7×10^6 (fig. 12(a)). (The peak heating at $x/L \approx 0.75$ for $R_{\infty,L} = 1.2 \times 10^6$ is not believed to be vortex-induced heating since oil-flow patterns do not indicate the interaction of vortices with the lee surfaces in this region; for $R_{\infty,L} = 0.7 \times 10^6$, no heat-transfer data were obtainable below $h/h_{ref} \approx 0.012$ since the phase-change paint did not melt below this value.) A "threshold" Reynolds number exists, in this instance based on body length, between 1.2×10^6 and 2.2×10^6 where peak heating decreases abruptly. Oil-flow studies, not shown herein, at these lower Reynolds numbers still exhibit the featherlike reattachment regions identified at the higher Reynolds

numbers. Therefore, the lack of peak heating and the existence of a threshold Reynolds number cannot be attributed to an elimination of the lee-side vortices. At $\alpha = 35^{\circ}$, the test Reynolds numbers for the smaller model are apparently above the threshold for that angle of attack since no abrupt decrease in peak heating was observed with decreasing Reynolds number. The presence of a threshold Reynolds number may well offer one of many explanations of why some investigators have failed to detect vortex-induced peak heating.

The variation in magnitude and location of the vortex-induced peak heating with body-length Reynolds number is presented in figure 14. Although the peak heating increases significantly with Reynolds number, the location of the heating peaks is relatively insensitive to Reynolds number. Note also that even though the relative nose bluntness (r/L) for the small-scale orbiter was half as large as that for the 0.00635-scale model, very little effect was observed on the magnitude or position of peak heating for Reynolds numbers above the threshold. Therefore, vortex-induced peak heating for the present delta-wing orbiter is concluded to be a weak function of nose bluntness for Reynolds numbers above the threshold. However, nose bluntness apparently influenced the threshold Reynolds number since the data at $\alpha = 20^{\circ}$ indicate that a threshold occurred only for the smaller scale model with a relatively smaller nose bluntness.

An analysis of the heating data in terms of boundary-layer properties and flow phenomena is difficult when heating is reduced only in the form of h/h_{ref} since h_{ref} is primarily useful in evaluating laminar heating for attached flows. Therefore, figure 15 presents the variation of the vortex-induced peak heating in terms of the free-stream Stanton number in addition to h/h_{ref} as a function of the free-stream Reynolds number based on the distance to the position of peak heating $(R_{\infty,x})$. Although the peak h/h_{ref} increases significantly with $R_{\infty,x}$, the peak heating in terms of Stanton number for a constant angle of attack is a relatively weak function of Reynolds number and increases only slightly. It should be emphasized that all the peaks were obtained at conditions above the threshold Reynolds number, in this instance based on distance to peak heating. In figure 16, for an angle of attack of 20°, a maximum heating for the vortex-influenced area beyond the attached flow region on the nose, $0.1 < x/L < 0.5$ (fig. 12(a)), is shown for the test conditions $\left(R_{\infty,x} \approx 0.25 \times 10^6 \text{ and } 0.4 \times 10^6\right)$ below the threshold where no peak occurred. A somewhat similar heating behavior has been observed with decreasing Reynolds number in the reattachment regions of separated boundary layers when the reattaching flow is transitional (ref. 15). Although the analogy between reattachment heating and vortex-induced heating should not be extended too far, the observed Reynolds number behavior suggests that the flow in the region of peak heating for these tests is transitional; the rapid decrease in heating with further reductions in Reynolds number is associated with the flow (not necessarily on the surface) becoming laminar. One might suppose that the Reynolds numbers are too low for transitional flow to occur;

however, some vortices are known to be highly unstable and thus may produce transitional flow at relatively low Reynolds numbers somewhat similar to that for wake flow (ref. 16). Furthermore, pressures measured along the lee meridian (fig. 13) increase with decreasing Reynolds numbers, a trend opposite in behavior with heating and characteristic of transitional flow reattachment (ref. 14). Further studies are necessary to determine both the specific cause of the rapid decrease in heating below the threshold and the parameter on which to define this threshold Reynolds number.

Effect of Mach Number

Lee-surface heating obtained at both Mach 19 and Mach 6 on the 0.00397-scale delta-wing orbiter are shown for $R_{\infty,L} \approx 0.7 \times 10^6$ in figure 17. No vortex-induced heating peaks (as opposed to maximum heating on the nose) for $x/L < 0.5$ were found for either $\alpha = 20^\circ$ or $\alpha = 37^\circ$ at Mach 19, and the heating level was significantly lower than that for $\alpha = 0^\circ$. The heating was also lower than that found at Mach 6. Unpublished oil-flow patterns at Mach 19 were found to be similar to those at Mach 6 with the exception that the featherlike signature, characteristic of vortex flows, was not clearly defined. This should not necessarily be attributed to the lack of lee-surface vortices since the surface shear may have been too low to move the oil and, hence, the characteristic featherlike pattern would not be formed. Since no peak heating occurred, the Reynolds number for the Mach 19 data was undoubtedly below the threshold. This is a reasonable conclusion since the Mach 19 Reynolds number $R_{\infty,L}$ was below the Mach 6 threshold value for $\alpha = 20^\circ$ and the local Reynolds numbers at Mach 19 were, of course, much lower than those at Mach 6. These high Mach number results are not sufficient to define the effect of Mach number since the influence of Reynolds number complicates the analysis. Additional studies to determine the Mach number effect are necessary since the effect of Mach number is required for an application of wind-tunnel results to flight conditions.

Effect of Geometry

The significant effect of configuration geometry on the magnitude and distribution of the lee-surface heating and surface flow is apparent by comparing figures 4 and 18. (Figure 19 summarizes the comparison of the heating.) The limited oil-flow and heating studies on the straight-wing orbiter show that vortices and vortex-induced heating are present on the lee side. However, the maximum heating peaks on the straight-wing orbiter occur at zero angle of attack and are a result of the canopy-induced shock-boundary-layer interaction over the forward portion of the fuselage, and transition and the dorsal fin over the aft portion. In contrast, the maximum heating on the delta-wing orbiter (compared with that on the straight-wing orbiter in fig. 19) occurred at $\alpha = 50^\circ$ as a result of the vortex-surface interaction. The important point to emphasize is that

a gross difference in configuration geometry can significantly affect the vortex-induced heating on the shuttle orbiter.

Although complete knowledge of the influence of lee-surface geometry is not presently available, simple variations in the lee-surface geometry strongly influence the vortex-induced heating. Dramatic reductions in the vortex-induced heating have been realized by altering the planform shape and lee-surface geometry of several planar delta wings at low incidence (refs. 12 and 17). The potential of varying the lee-surface geometry on the shuttle to reduce heating is shown for several configurations at Mach 6 and 8 in figure 20. The Mach 6 data show the results of a modification to the existing delta-wing orbiter model. The rationale behind this modification primarily involved the alteration of the lee-surface geometry to encourage the vortices, if present, to break away from the lee surface. The initial slope of the lee meridian was increased and broken sharply with the hope that the vortices would lift off the surface at the geometry discontinuity. As the data reveal, the heating level was reduced significantly over a major portion of the leeward meridian. (No heating data were obtained on the modified configuration beyond $x/L \approx 0.33$ and below $h/h_{ref} \approx 0.095$ since the phase-change paint did not melt beyond these points.)

Further verification of the concept of reducing lee-surface heating by modifying the upper surface geometry to induce vortex lift-off can be found by comparing reference 3 with unpublished data obtained in the Langley Mach 8 variable-density hypersonic tunnel by H. D. Schultz and K. W. McGee of Lockheed Missiles & Space Company. The profiles of the orbiters tested at Mach 8 are shown in figure 20. The configuration of Schultz and McGee with relatively large initial slope angle and sharp break in contour generated relatively low lee-surface heating in comparison with the configuration of Connor, which had a more gradually changing contour. Therefore, it seems advantageous in terms of heating to shape the upper surface of the shuttle with a relatively large initial slope that breaks sharply to encourage vortex lift-off. Although some of the current shuttle concepts utilize profiles somewhat similar to those which produced the lower lee-surface heating, additional guidelines for configuring the shuttle to insure reductions in vortex-induced heating are needed.

Application of Wind-Tunnel Results to Flight Environments

Lee-surface vortex-induced heating should be expected on some of the conceptual shuttle configurations in flight. However, it is difficult to determine quantitatively the severity of the vortex-induced heating since the heating is influenced by numerous interrelated parameters (i.e., Mach number, Reynolds number, angle of attack, geometry, and probably real-gas effects and wall cooling). Furthermore, this complicated interrelation of parameters precludes satisfactory theoretical heating predictions at this time.

Application of the present wind-tunnel results at Mach 6 and 19 to projected shuttle flight trajectories (ref. 13) is instructive in indicating the severity of the lee-surface heating in flight. (See fig. 21.) The radiation equilibrium surface temperatures were calculated for the maximum vortex-induced heating rates obtained experimentally on the lee surface of the 0.00397-scale delta-wing orbiter at $\alpha = 20^{\circ}$ for several Reynolds numbers. The maximum stagnation heat-transfer rate used in the calculation of surface temperatures was assumed to be 136 kW/m^2 for Mach 6 and 790 kW/m^2 for Mach 19 based on typical high-cross-range trajectories (ref. 13). At the higher Reynolds numbers at Mach 6, which are approaching the projected flight Reynolds numbers, the surface temperatures are significantly greater than the established structural limit for titanium. Below the threshold Reynolds number, however, the surface temperatures are appreciably lower. The insert of figure 21 shows the important influence of threshold Reynolds number on the surface temperatures.

At Mach 19, the surface temperatures for $R_{\infty,L} = 0.7 \times 10^6$ were below the structural limit for titanium; undoubtedly, this Reynolds number was below the threshold Reynolds number for the particular test conditions. Although it is not known how much the Mach 19 conditions were below the threshold Reynolds number, application of the experimental Mach 6 Reynolds number effects on peak heating to the expected flight Reynolds numbers and Mach numbers (fig. 22) indicates that the most severe vortex-induced heating will occur at the lower hypersonic Mach numbers (e.g., Mach 7 to 15). The rather conservative assumptions made to obtain this conclusion are indicated in figure 22. Since the lee-surface heating problem is extremely complex, completely definitive studies of lee-surface heating throughout the Mach number range cannot be obtained until the shuttle geometries have been partially fixed. However, utilization of lee-surface shaping guidelines, which are now under development, is recommended for the reduction of vortex-induced lee-surface heating.

CONCLUSIONS

Results of a continuing experimental lee-surface heating investigation at Mach numbers of 6 and 19 on two conceptual space shuttle orbiters have been presented with the following conclusions:

1. The severity of vortex-induced lee-surface heating is strongly influenced by Reynolds number, and there exists a threshold Reynolds number below which peak heating decreases abruptly with decreasing Reynolds number.

2. Relatively low lee-surface heating was found for the test conditions at Mach 19 which were undoubtedly below the threshold Reynolds number. However, these results

were insufficient to define Mach number effects on heating since the Reynolds number influence is interrelated with Mach number.

3. Vortex-induced peak heating is a relatively weak function of nose bluntness for Reynolds numbers above the threshold. A variation in nose bluntness by a factor of 2 had little effect on the magnitude or position of peak heating. However, the data indicate that nose bluntness influences the threshold Reynolds number.

4. Variations in lee-surface geometry strongly influence vortex-induced peak heating. Modifying upper surface geometry to encourage vortex lift-off reduced the vortex-induced heating; additional guidelines to insure this reduction in heating are necessary.

5. At the position of peak heating, the pressures decrease slightly with increasing Reynolds number and remain nearly constant with increasing angle of attack. In contrast, the peak heating increased with Reynolds number and angle of attack.

6. Vortex-induced heating should be expected on the shuttle in flight with the most severe lee-surface heating probably occurring at the lower hypersonic Mach numbers. A quantitative determination of this heating is very difficult since it is influenced by numerous interrelated parameters; continuing research is indicated.

Langley Research Center,
National Aeronautics and Space Administration,
Hampton, Va., October 13, 1972.

REFERENCES

1. Hefner, Jerry N.; and Whitehead, Allen H., Jr.: Lee-Side Heating Investigations. Part I – Experimental Lee-Side Heating Studies on a Delta-Wing Orbiter. NASA Space Shuttle Technology Conference. NASA TM X-2272, 1971, pp. 267-287.

2. Hefner, Jerry N.; and Whitehead, Allen H., Jr.: Lee-Side Flow Phenomena on Space Shuttle Configurations at Hypersonic Speeds. Pt. II – Studies of Lee-Surface Heating at Hypersonic Mach Numbers. Space Shuttle Aerothermodynamics Technology Conference, Vol. II, NASA TM X-2507, 1972, pp. 451-467.

3. Connor, L. E.: Heat Transfer Tests of the Lockheed Space Shuttle Orbiter Configuration Conducted at the Langley Research Center Mach 8 Variable Density Tunnel. TM 54/20-241, Lockheed Missiles & Space Co., Dec. 1969.

4. Lockman, William K.; and DeRose, Charles E.: Aerodynamic Heating of a Space Shuttle Delta-Wing Orbiter. NASA TM X-62057, 1971.

5. Matthews, R. K.; Buchanan, T. D.; Martindale, W. R.; and Warmbrod, J. D.: Experimental and Theoretical Aerodynamic Heating and Flow Field Analysis of a Space Shuttle Orbiter. Space Shuttle Aerothermodynamics Technology Conference, Vol. II, NASA TM X-2507, 1972, pp. 261-296.

6. Jones, Robert A.; and Hunt, James L.: Use of Fusible Temperature Indicators for Obtaining Quantitative Heat-Transfer Data. NASA TR R-230, 1966.

7. Goldberg, Theodore J.; and Hefner, Jerry N. (With appendix by James C. Emery): Starting Phenomena for Hypersonic Inlets With Thick Turbulent Boundary Layers at Mach 6. NASA TN D-6280, 1971.

8. Beckwith, Ivan E.; Harvey, William D.; and Clark, Frank L. (With appendix A by Ivan E. Beckwith, William D. Harvey, and Christine M. Darden and appendix B by William D. Harvey, Lemuel E. Forrest, and Frank L. Clark): Comparisons of Turbulent-Boundary-Layer Measurements at Mach Number 19.5 With Theory and an Assessment of Probe Errors. NASA TN D-6192, 1971.

9. Arrington, James P.; and Ashby, George C., Jr.: Effect of Configuration Modifications on the Hypersonic Aerodynamic Characteristics of a Blended Delta Wing-Body Entry Vehicle. NASA TM X-2611, 1972.

10. Stone, David R.: Aerodynamic Characteristics of a Fixed-Wing Manned Space Shuttle Concept at a Mach Number of 6.0. NASA TM X-2049, 1970.

11. Fay, J. A.; and Riddell, F. R.: Theory of Stagnation Point Heat Transfer in Dissociated Air. J. Aeronaut. Sci., vol. 25, no. 2, Feb. 1958, pp. 73-85, 121.

12. Whitehead, Allen H., Jr.; and Bertram, Mitchel H.: Alleviation of Vortex-Induced Heating to the Lee Side of Slender Wings in Hypersonic Flow. AIAA J., vol. 9, no. 9, Sept. 1971, pp. 1870-1872.

13. Arrington, James P.: Entry Maneuver/Aerothermodynamic Interactions for High Cross-Range Candidate Orbiters. Space Transportation System Technology Symposium, I – Aerothermodynamics and Configurations, NASA TM X-52876, Vol. I, 1970, pp. 509-530.

14. Hama, Francis R.: Experimental Investigations of Wedge Base Pressure and Lip Shock. Tech. Rep. No. 32-1033 (Contract No. NAS 7-100), Jet Propulsion Lab., California Inst. Technol., Dec. 1, 1966. (Available as NASA CR-81031.)

15. Holloway, Paul F.; Sterrett, James R.; and Creekmore, Helen S.: An Investigation of Heat Transfer Within Regions of Separated Flow at a Mach Number of 6.0. NASA TN D-3074, 1965.

16. Chang, Paul K.: Separation of Flow. Pergamon Press, Inc., c.1970, pp. 396-400.

17. Rao, Dhanvada Madhava: Hypersonic Lee-Surface Heating Alleviation on Delta Wing by Apex-Drooping. AIAA J., vol. 9, no. 9, Sept. 1971, pp. 1875-1876.

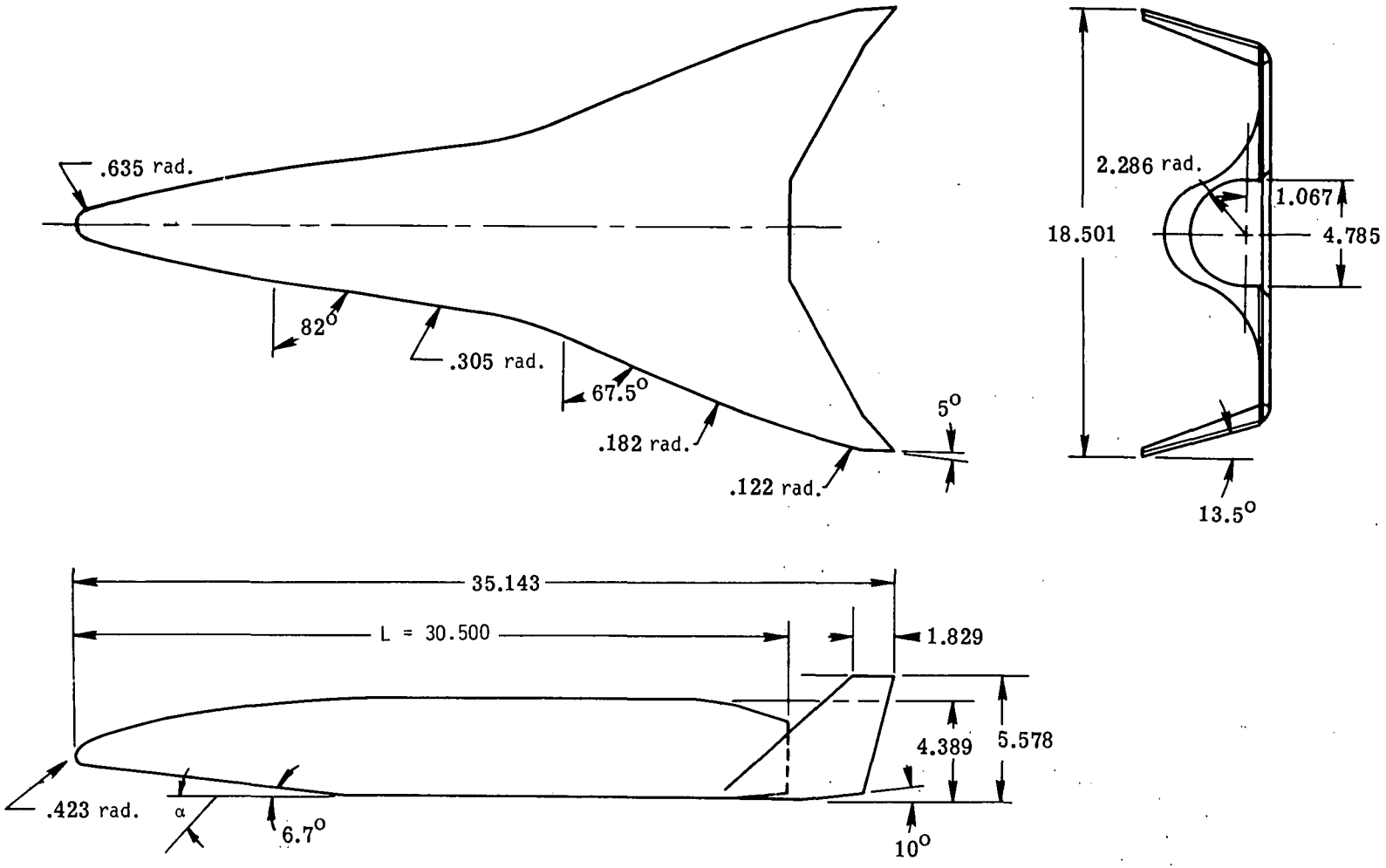

(a) 0.00635-scale delta-wing orbiter; r/L = 0.02.

Figure 1.- Drawing of wind-tunnel models. All dimensions are in centimeters.

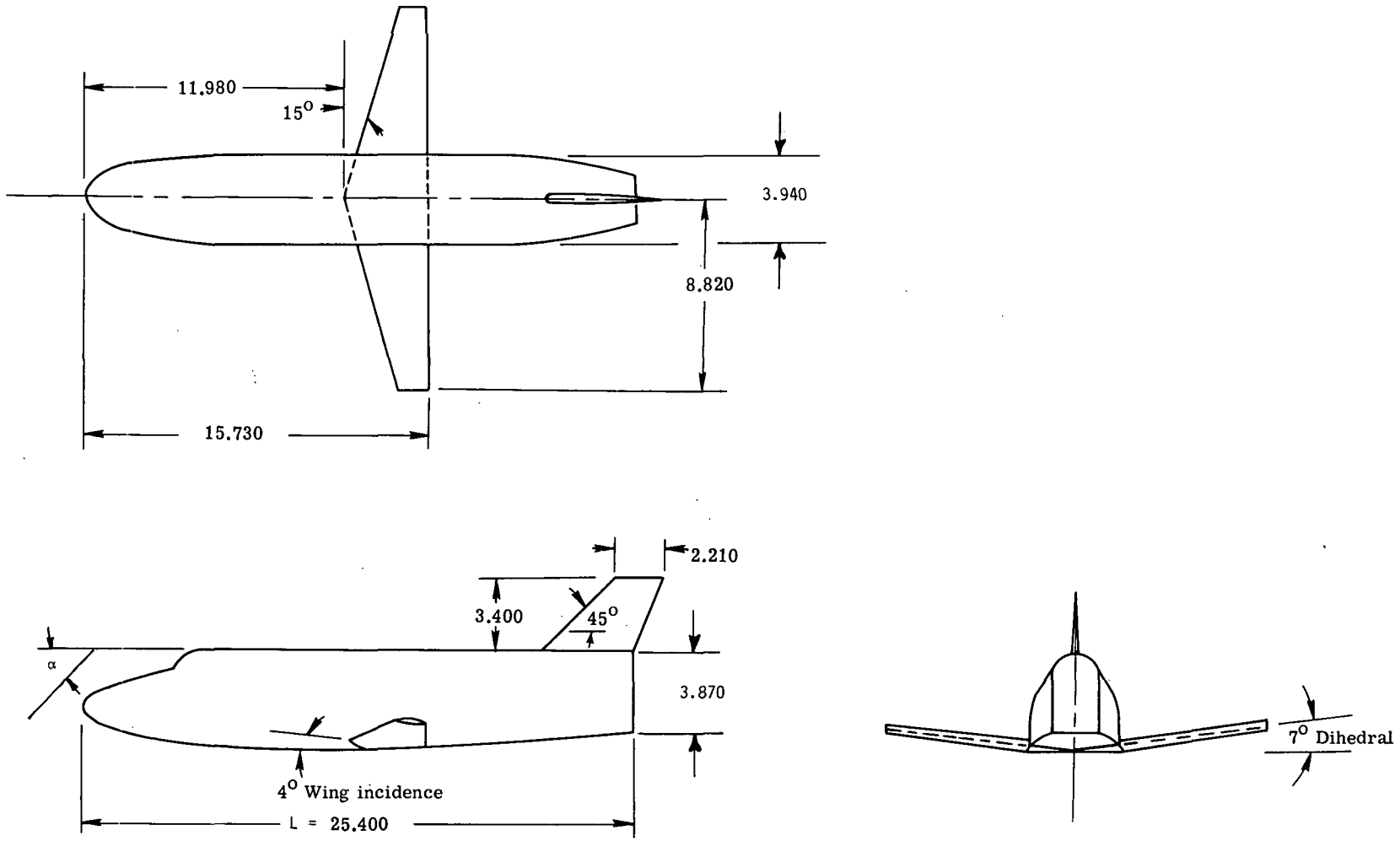

(b) 0.00725-scale straight-wing orbiter.

Figure 1.- Concluded.

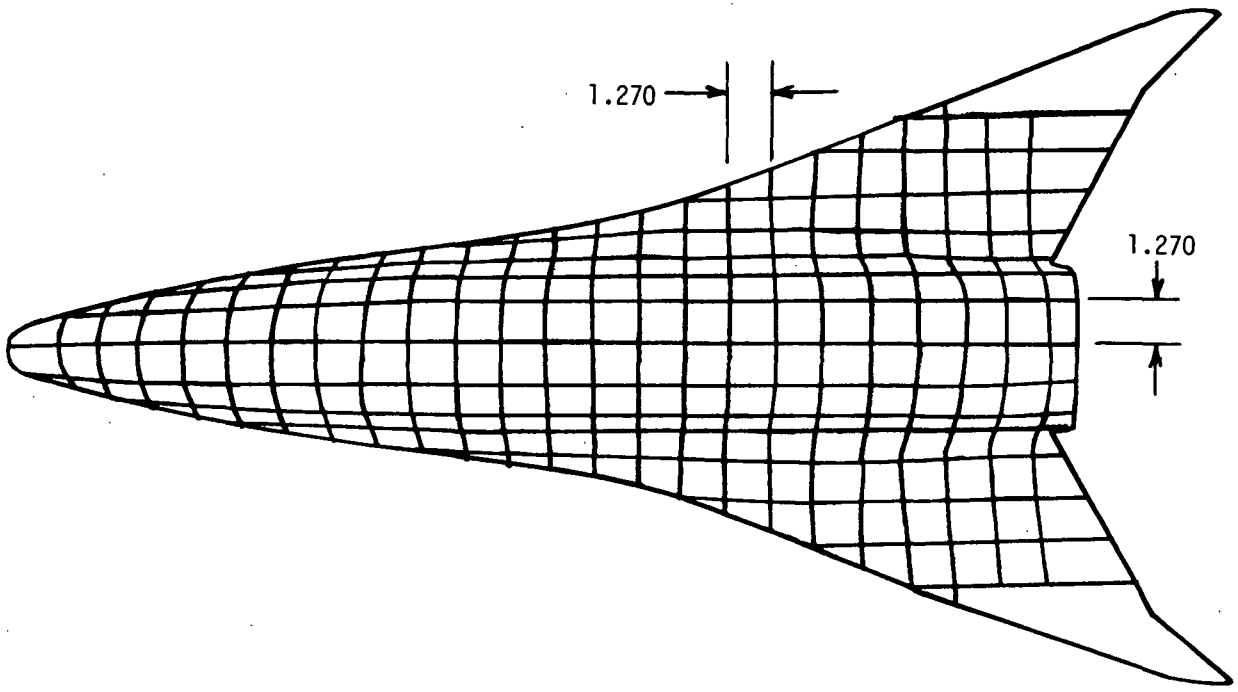

(a) 0.00635-scale delta-wing orbiter model.

Figure 2.- Grid characteristics for phase-change-paint models. All dimensions are in centimeters.

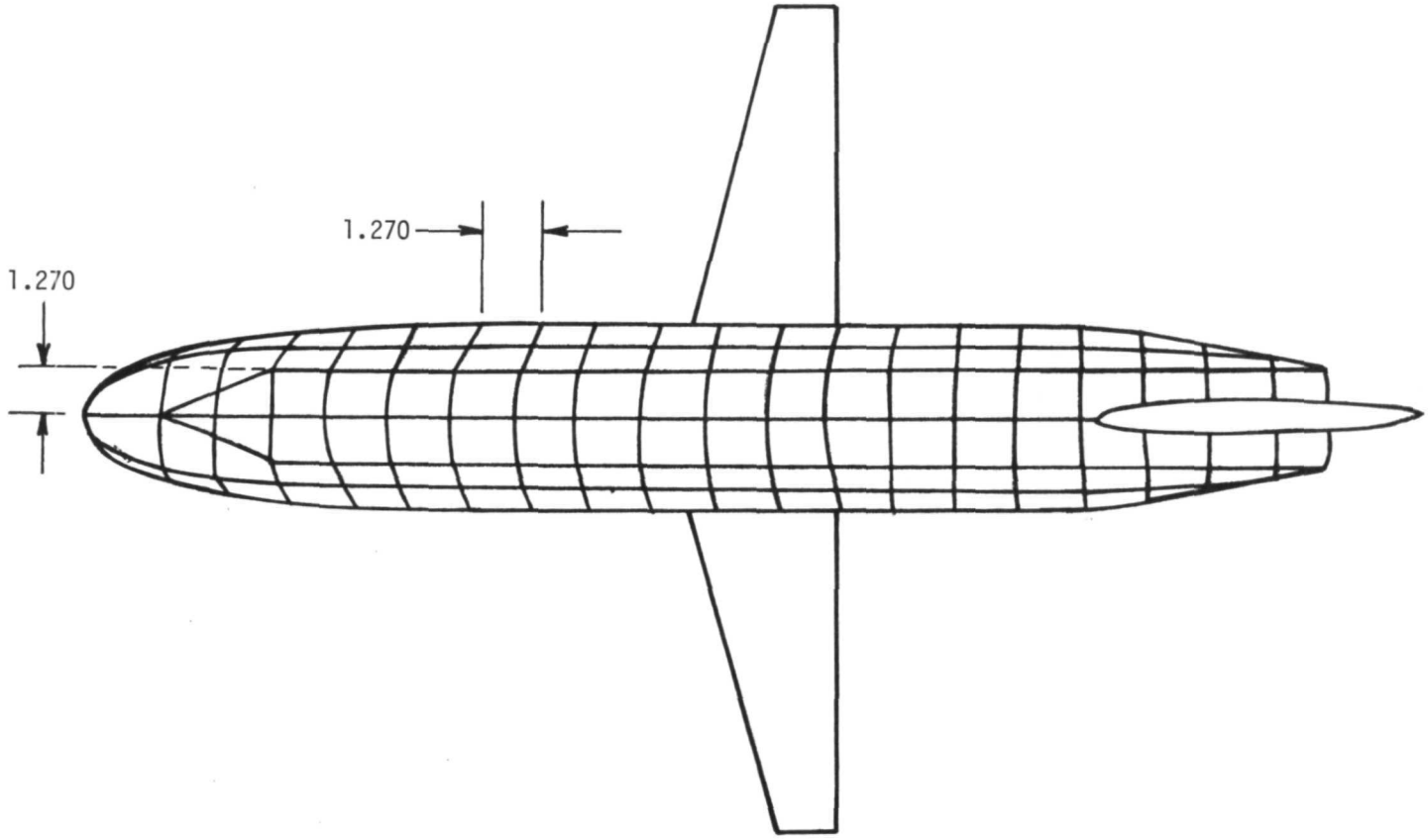

(b) 0.00725-scale straight-wing orbiter model.

Figure 2.- Concluded.

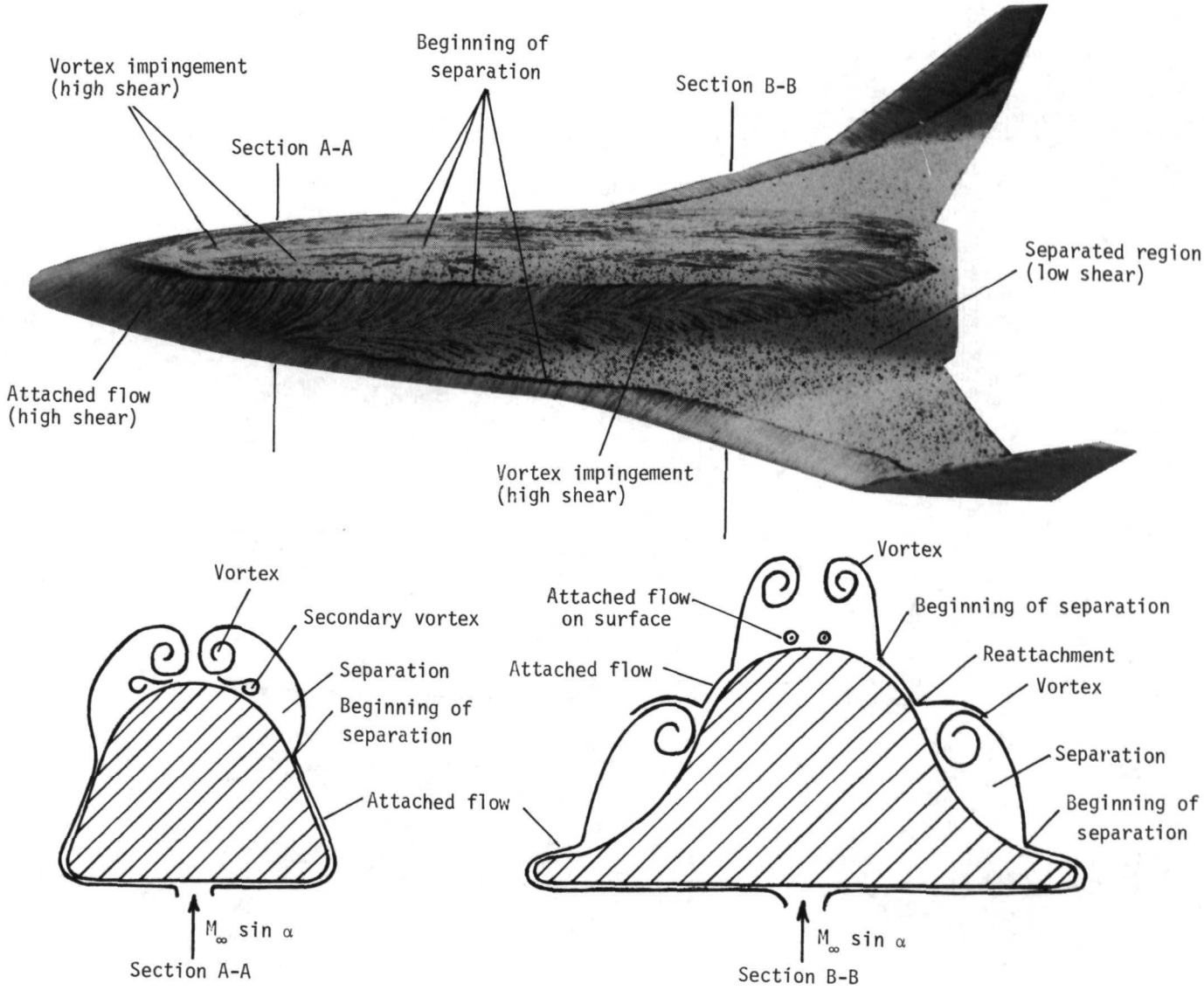

L-72-6540

Figure 3.- Lee-surface flow characteristics on delta-wing orbiter. $M_\infty = 6$; $\alpha = 20^o$.

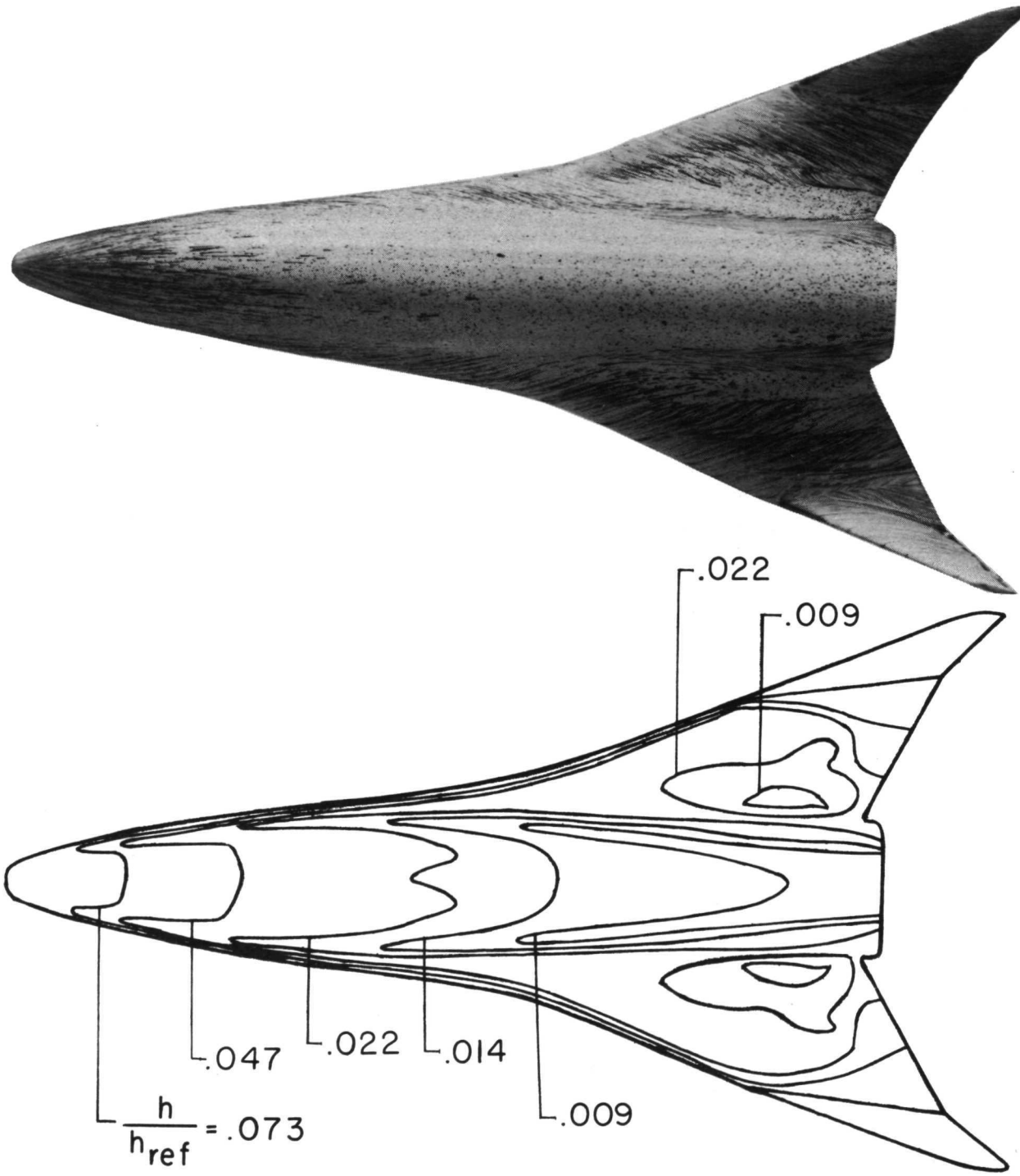

L-72-6541

(a) $\alpha = 0^{o}$.

Figure 4.- Surface flow and heating on 0.00635-scale delta-wing orbiter. $M_{\infty} = 6$; $R_{\infty,L} = 5.2 \times 10^{6}$.

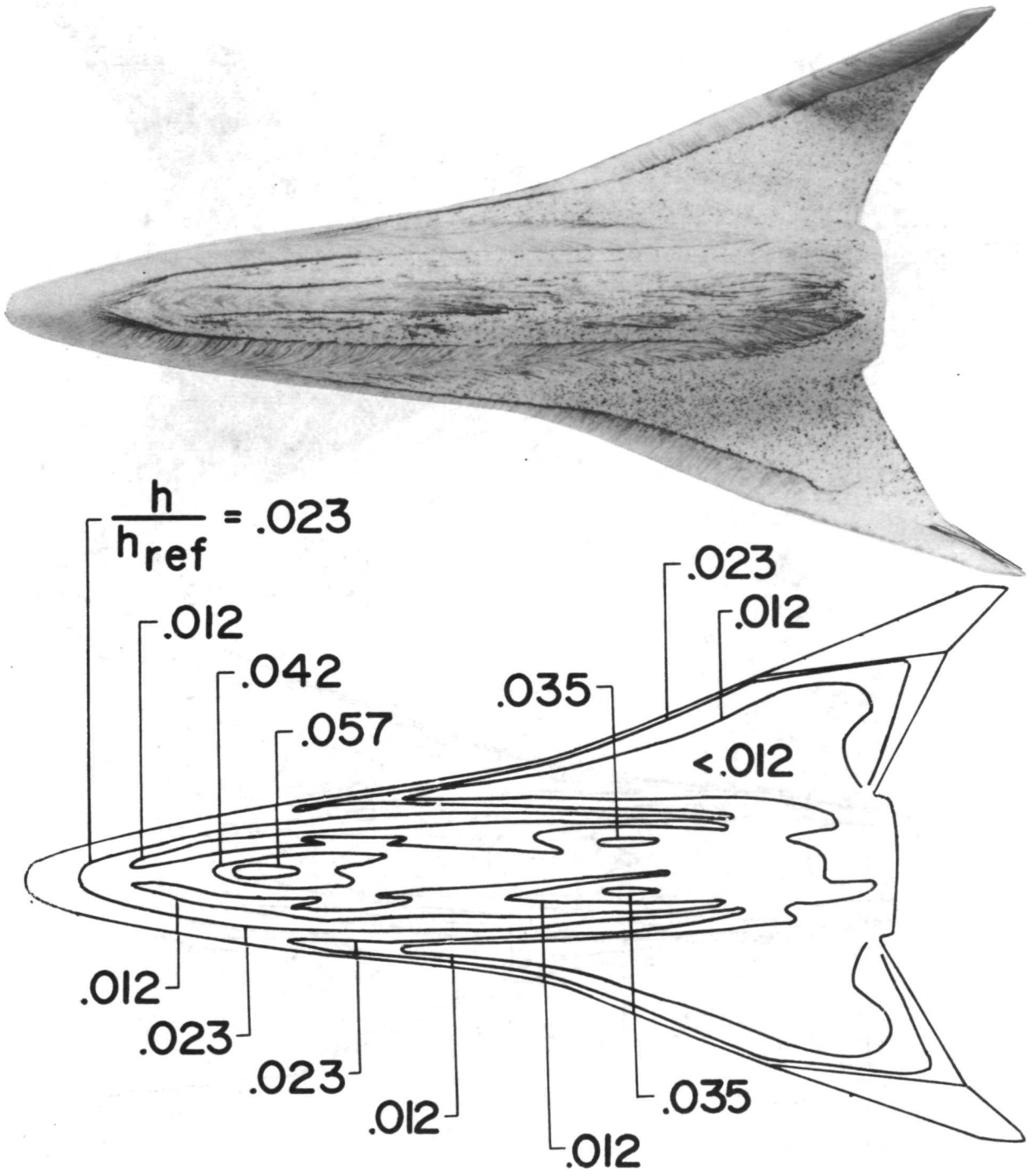

L-72-6542

(b) $\alpha = 20^{o}$.

Figure 4.- Continued.

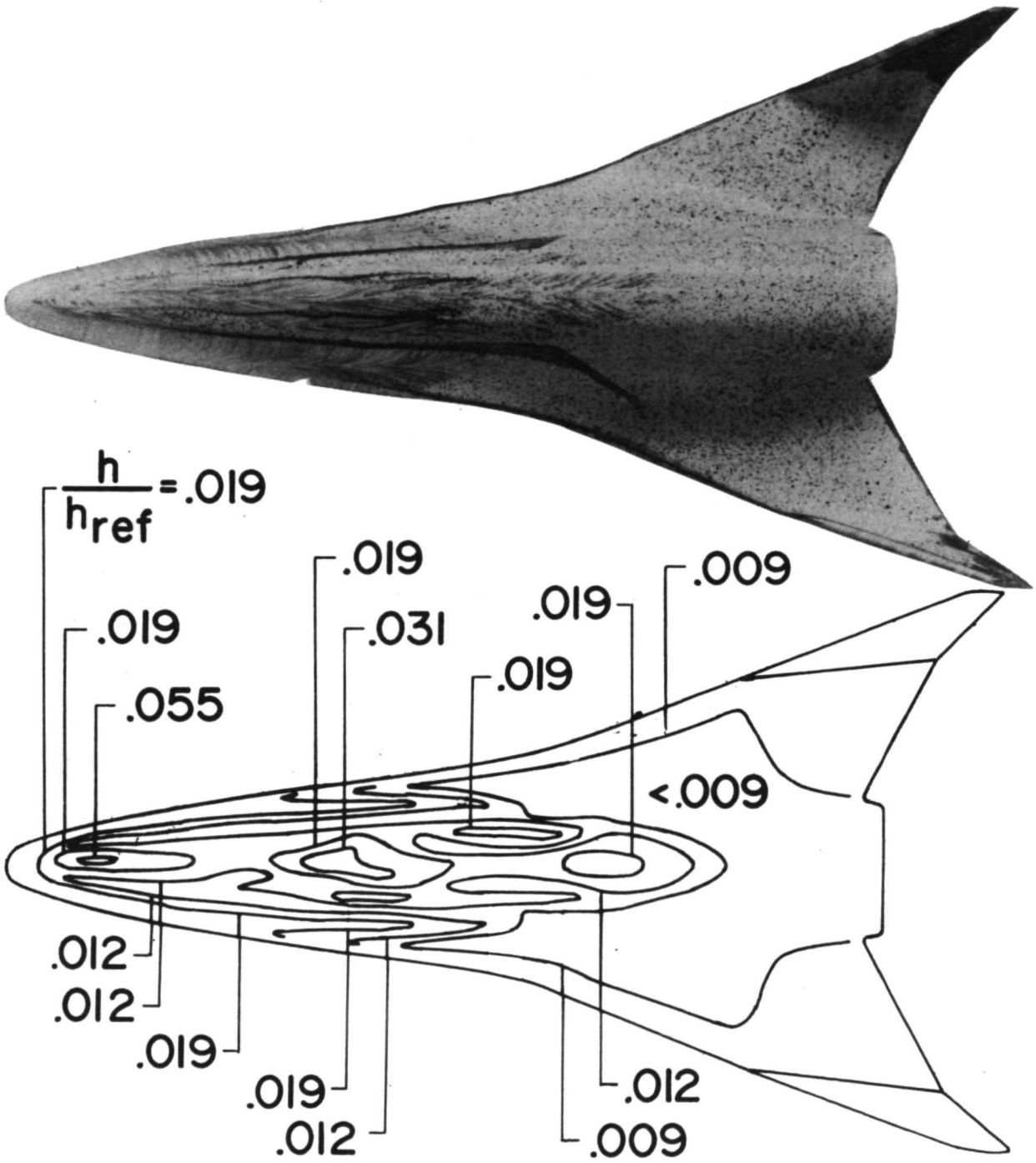

L-72-6543

(c) $\alpha = 40^{o}$.

Figure 4.- Continued.

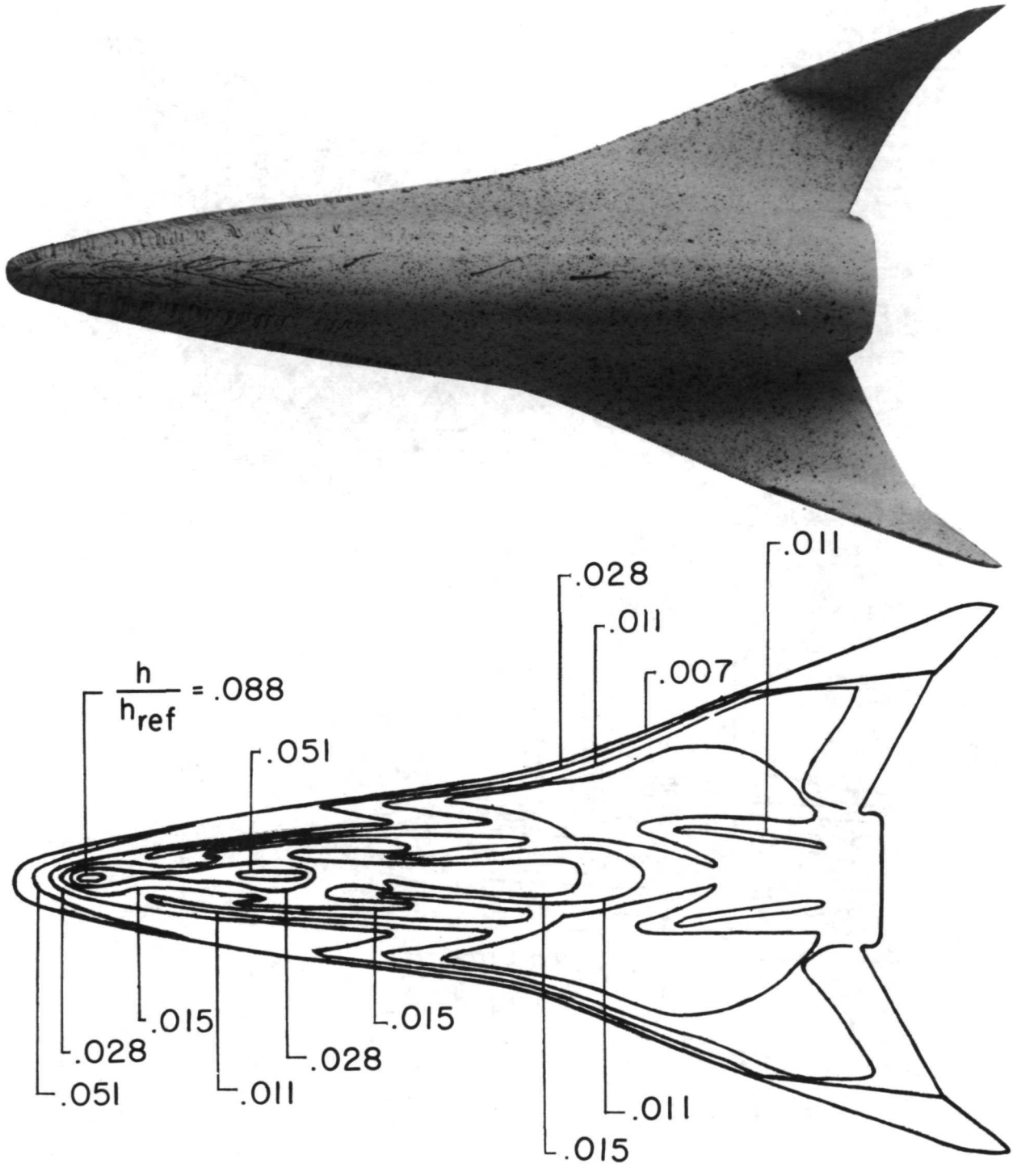

L-72-6544

(d) $\alpha = 50^{o}$.

Figure 4.- Concluded.

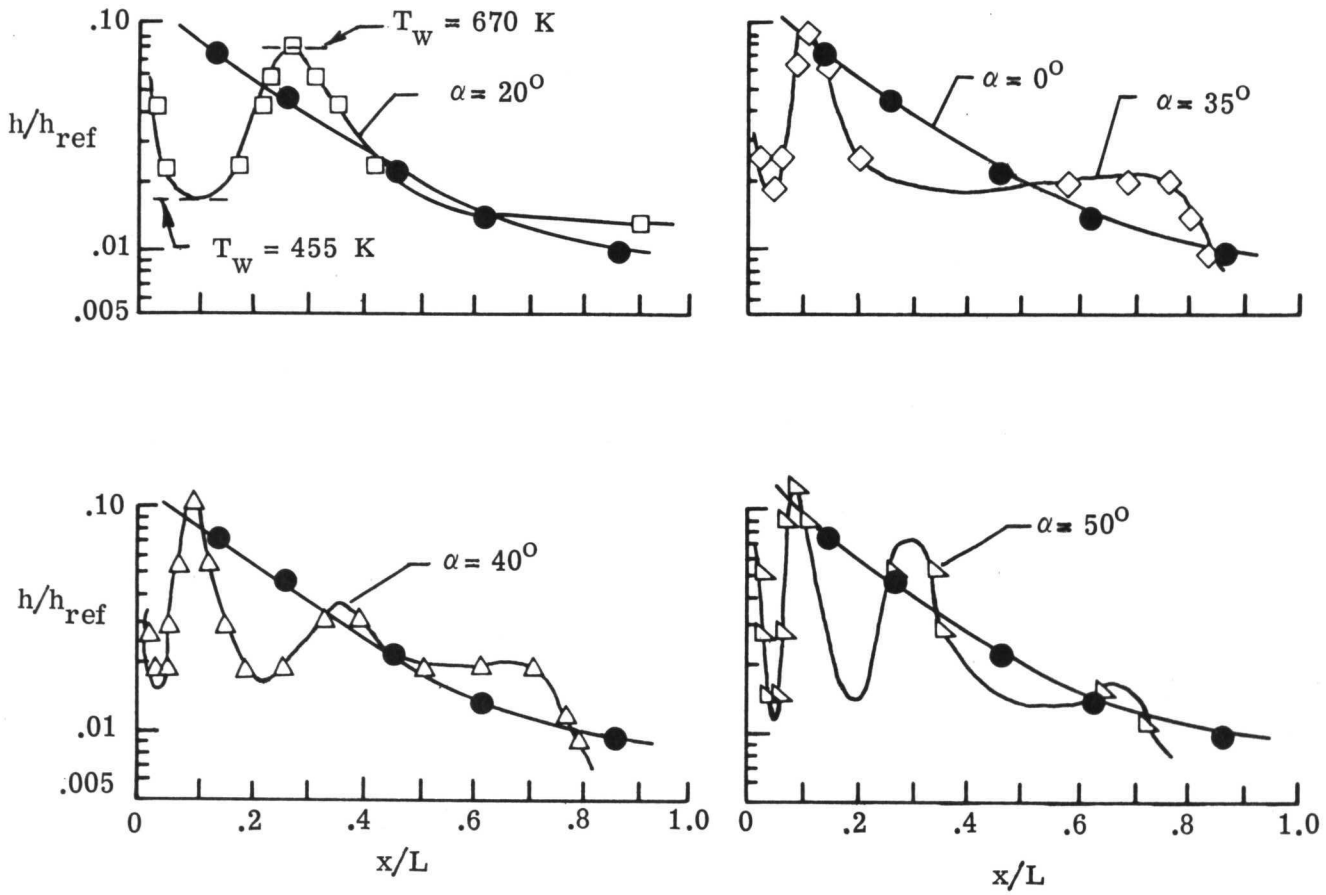

Figure 5.- Heating along lee-surface meridian of 0.00635-scale delta-wing orbiter at angle of attack. $M_\infty = 6$; $R_{\infty,L} = 5.2 \times 10^6$.

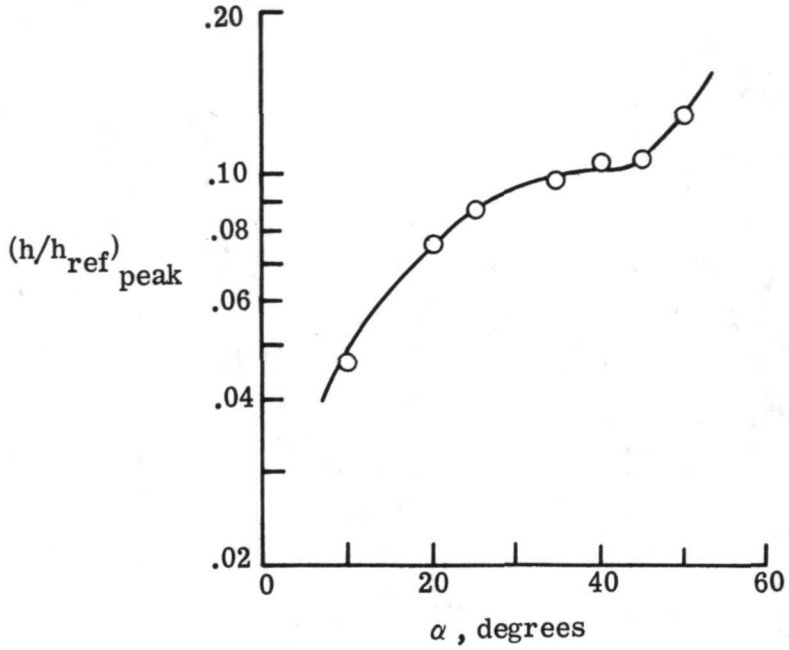

(a) Peak heating.

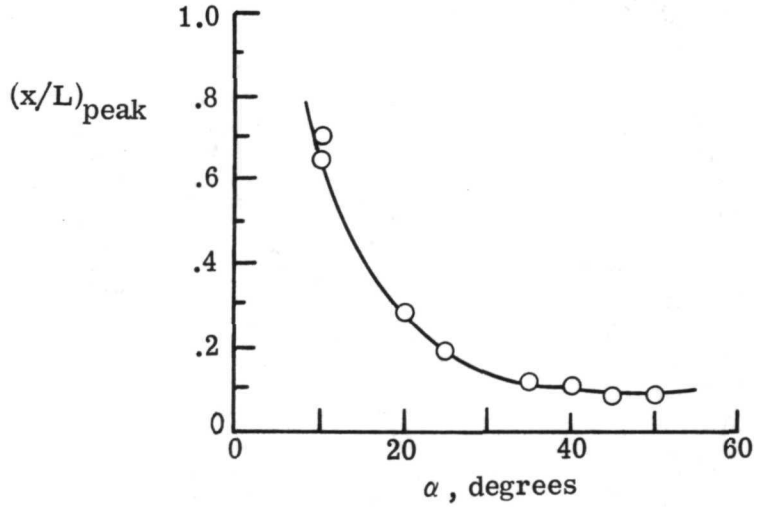

(b) Location of peak heating.

Figure 6.- Effect of angle of attack on lee-meridian peak heating for 0.00635-scale delta-wing orbiter. $M_\infty = 6$; $R_{\infty,L} = 5.2 \times 10^6$.

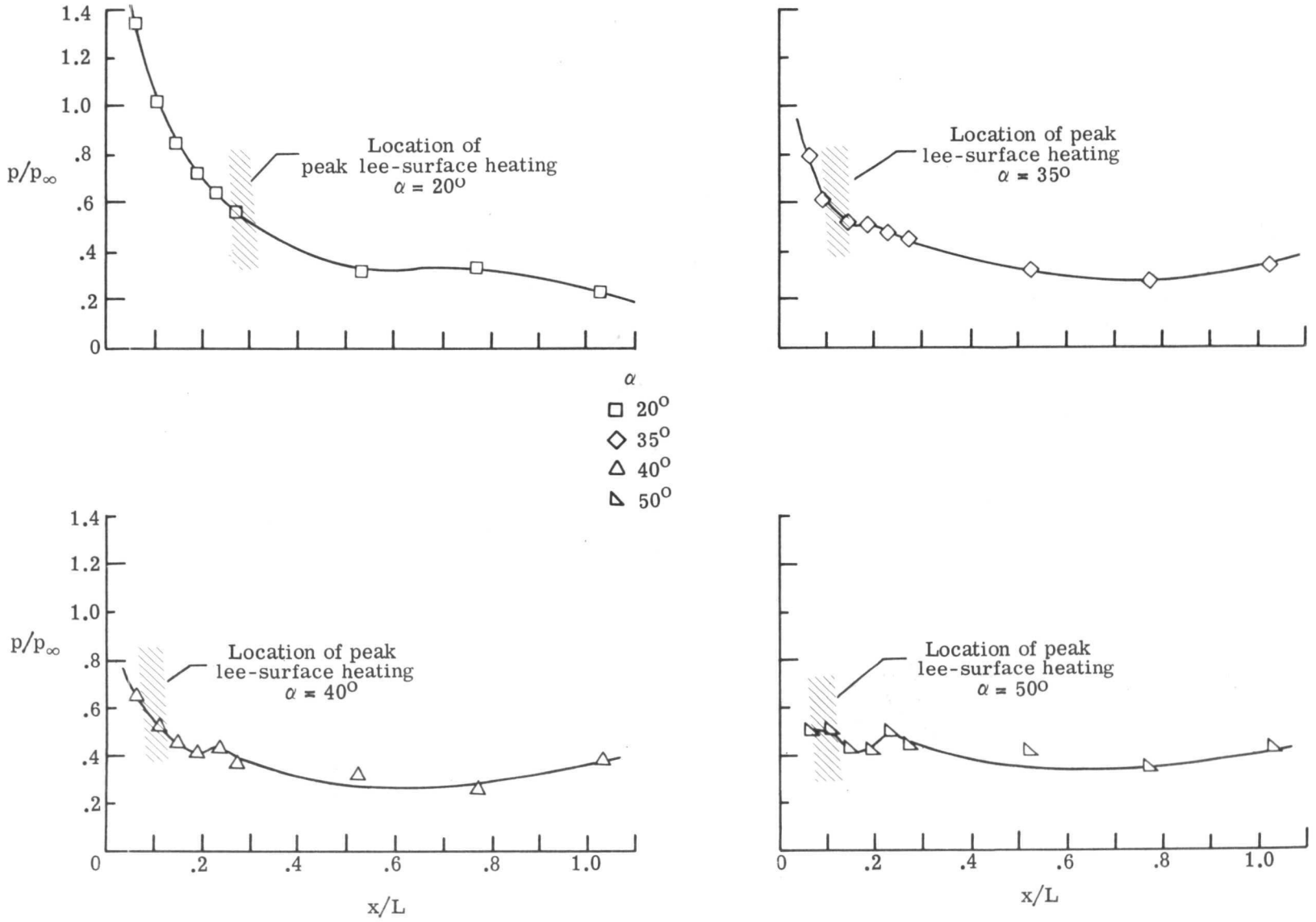

Figure 7.- Pressure distribution on lee meridian of 0.00635-scale delta-wing orbiter. $M_\infty = 6$; $R_{\infty,L} = 5.2 \times 10^6$.

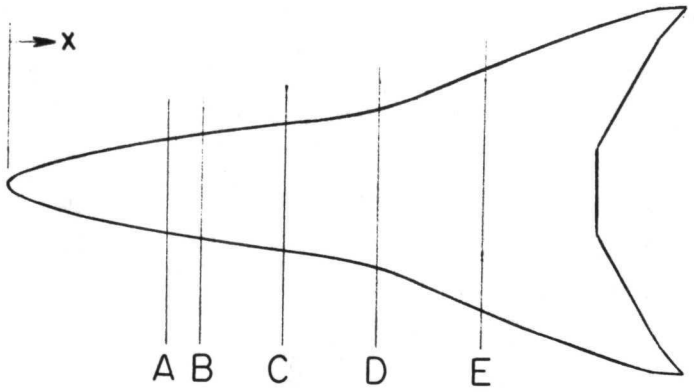

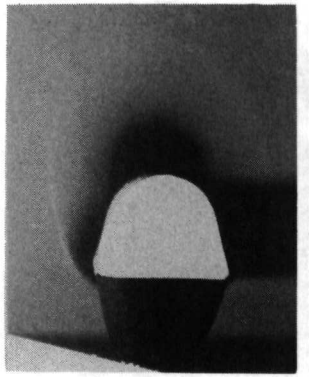

A. $\frac{x}{L} = 0.27$

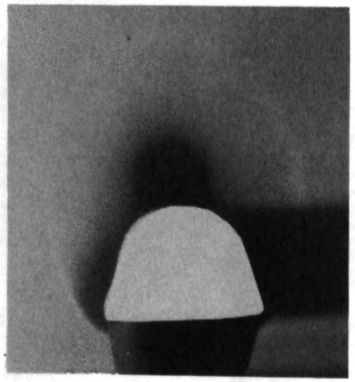

B. $\frac{x}{L} = 0.33$

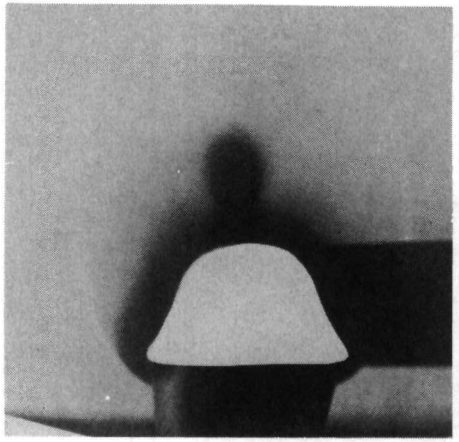

C. $\frac{x}{L} = 0.47$

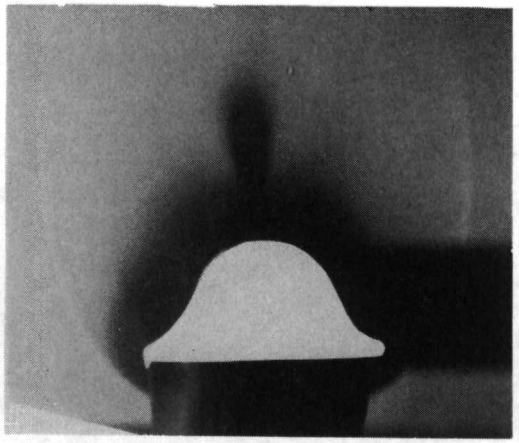

D. $\frac{x}{L} = 0.63$

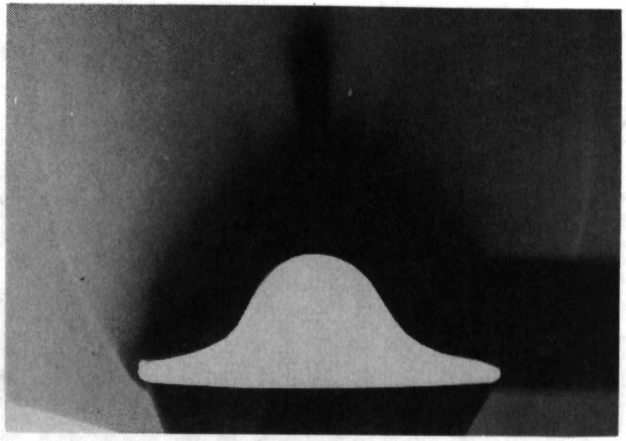

E. $\frac{x}{L} = 0.81$

L-72-6545

Figure 8.- Vapor-screen photograph of 0.00635-scale delta-wing orbiter. $M_\infty = 6$; $\alpha = 20^o$; $R_{\infty,L} = 5.2 \times 10^6$.

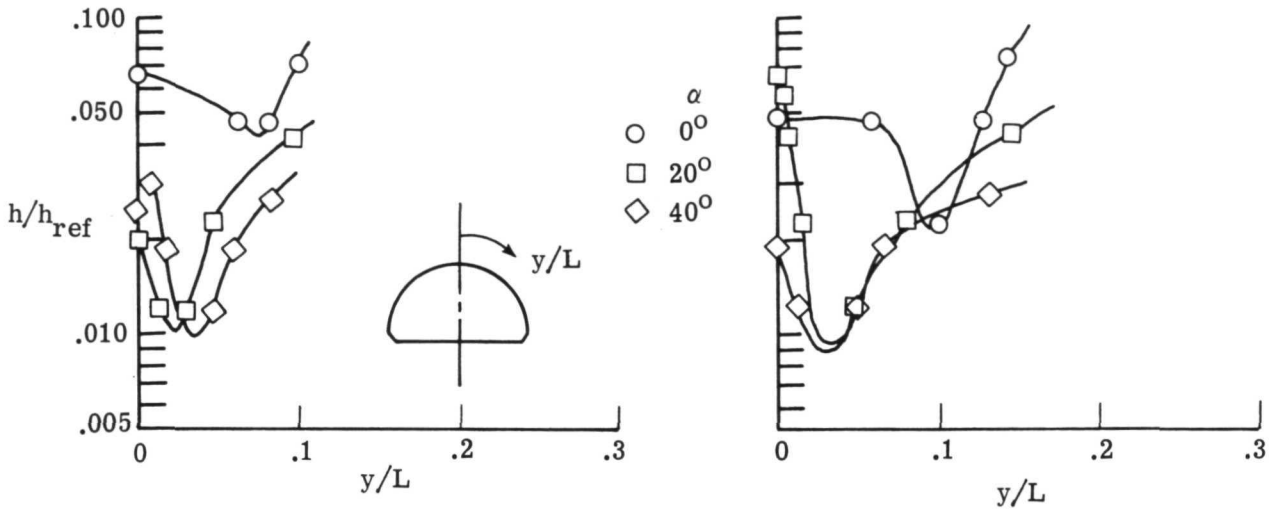

(a) x/L = 0.167.

(b) x/L = 0.250.

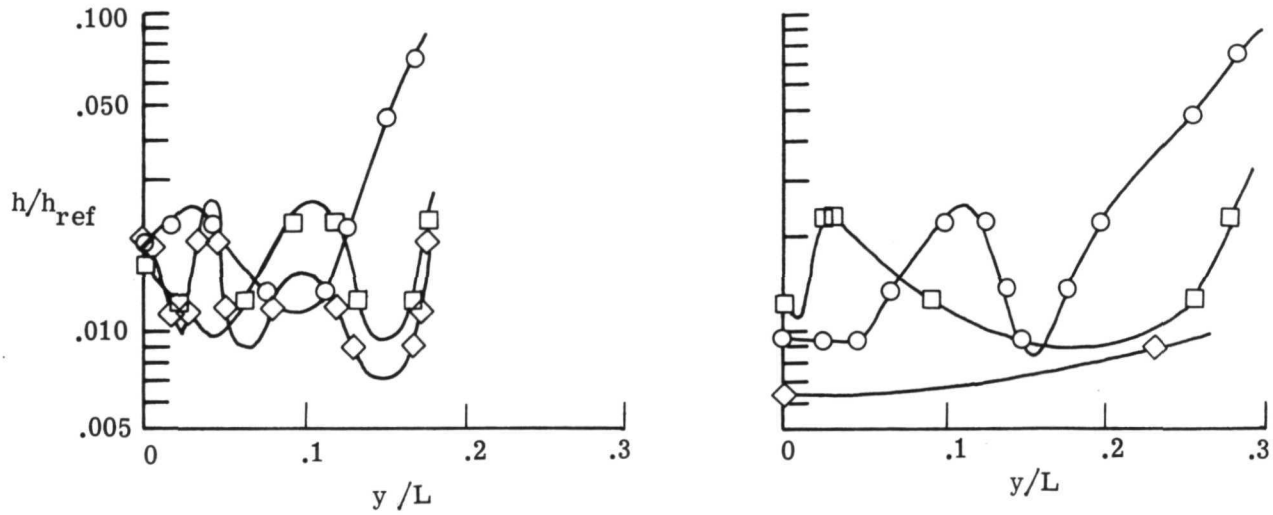

(c) x/L = 0.500.

(d) x/L = 0.833.

Figure 9.- Spanwise heating distribution on lee surface of 0.00635-scale delta-wing orbiter. $M_\infty = 6$; $R_{\infty,L} = 5.2 \times 10^6$.

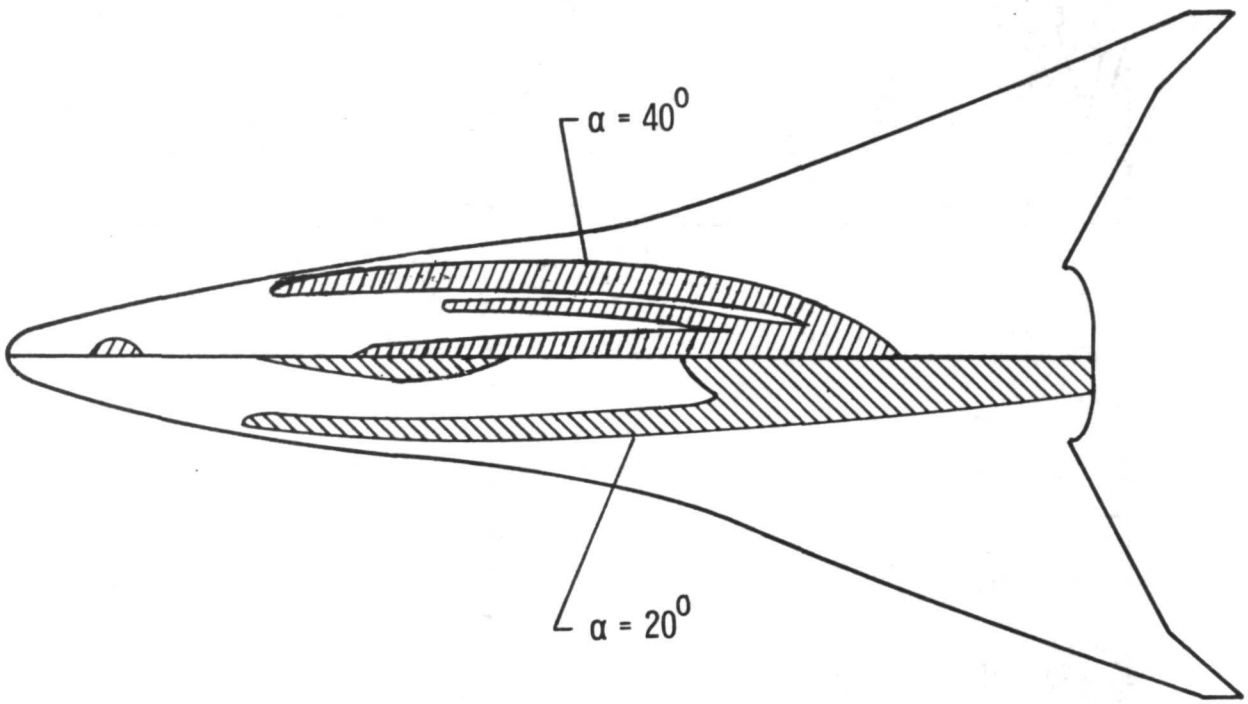

Figure 10.- Regions of increased heating on lee surface of 0.00635-scale delta-wing orbiter. $M_\infty = 6$; $R_{\infty,L} = 5.2 \times 10^6$.

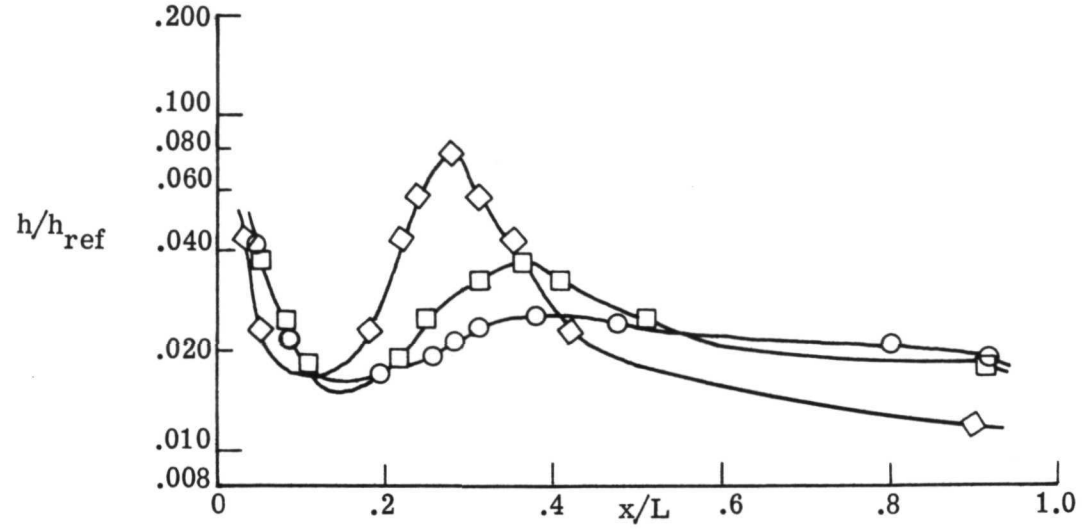

(a) $\alpha = 20^{o}$.

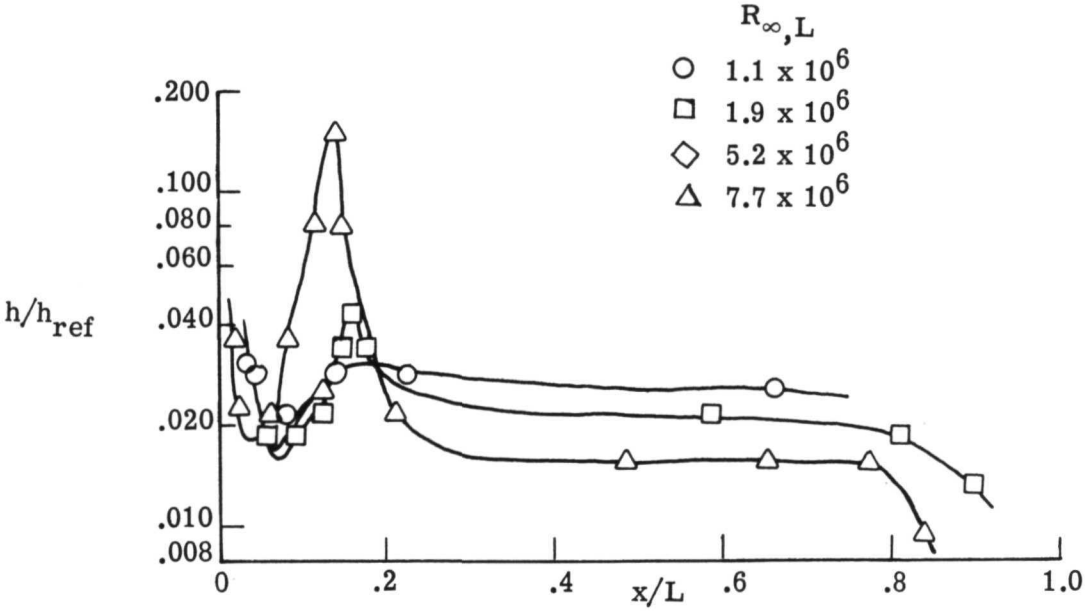

(b) $\alpha = 35^{o}$.

Figure 11.- Variation in heating with Reynolds number for 0.00635-scale delta-wing orbiter.

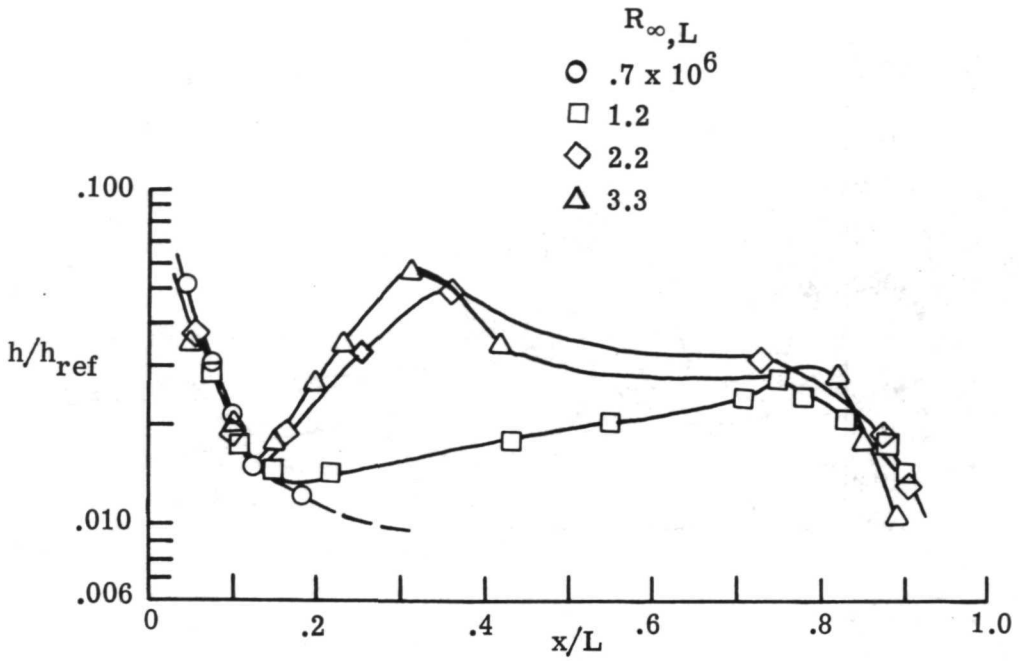

(a) $\alpha = 20^{\circ}$.

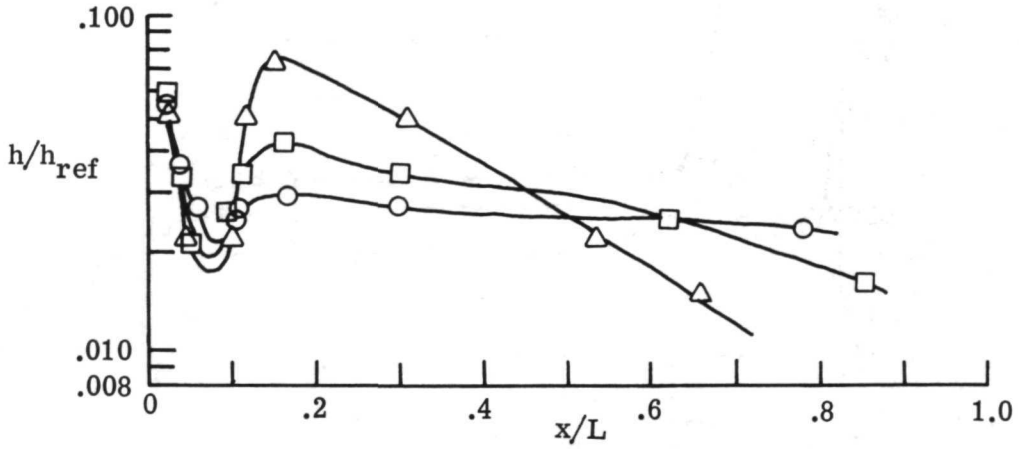

(b) $\alpha = 35^{\circ}$.

Figure 12.- Variation in heating with Reynolds number for 0.00397-scale delta-wing orbiter.

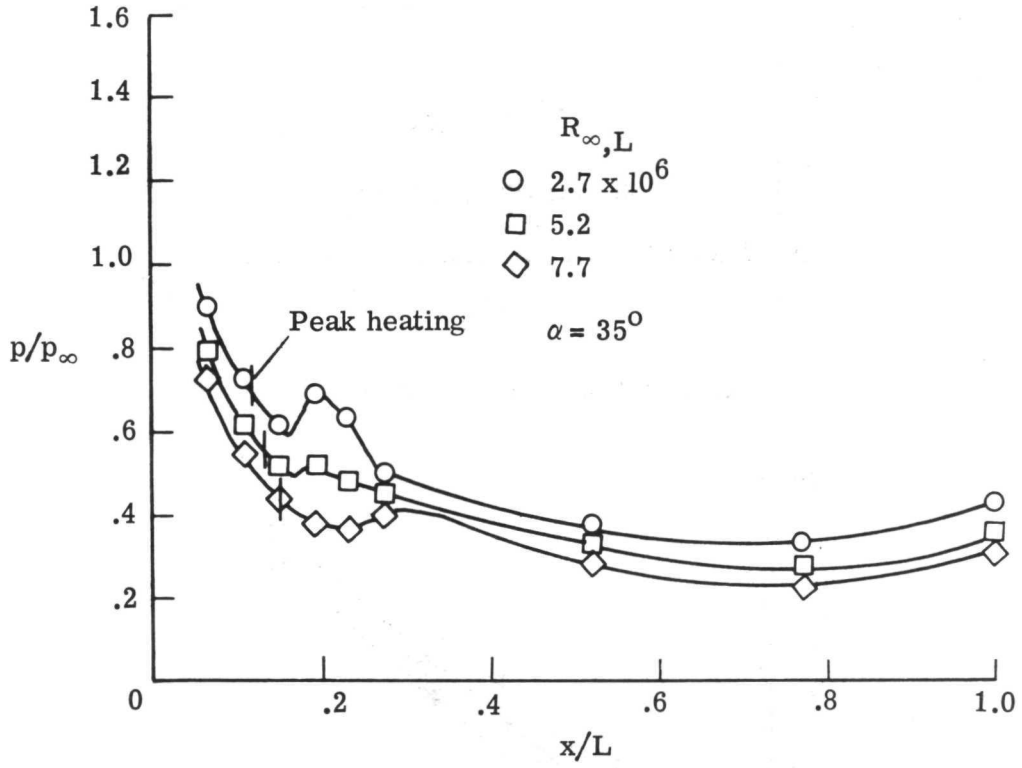

Figure 13.- Variation of lee-meridian pressure distribution with Reynolds number for 0.00635-scale delta-wing orbiter. $M_\infty = 6$.

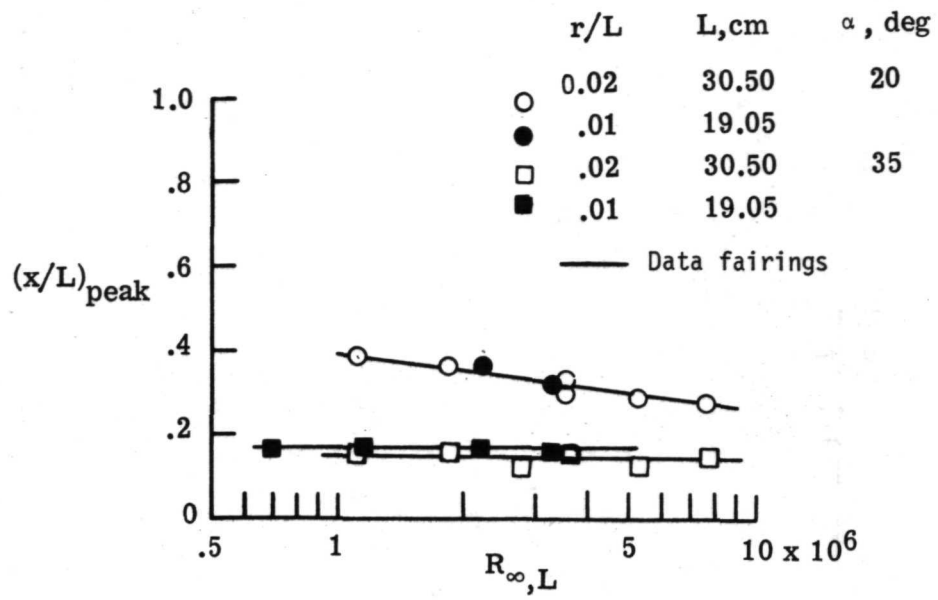

(a) Location of peak heating.

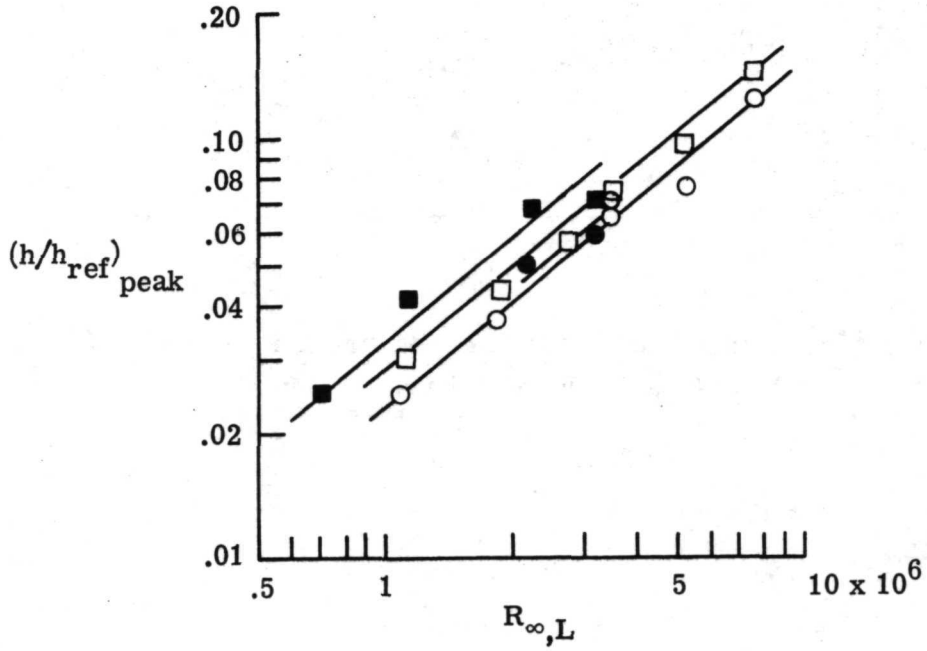

(b) Peak heating.

Figure 14.- Effect of Reynolds number on peak heating on delta-wing orbiter. $M_\infty = 6$.

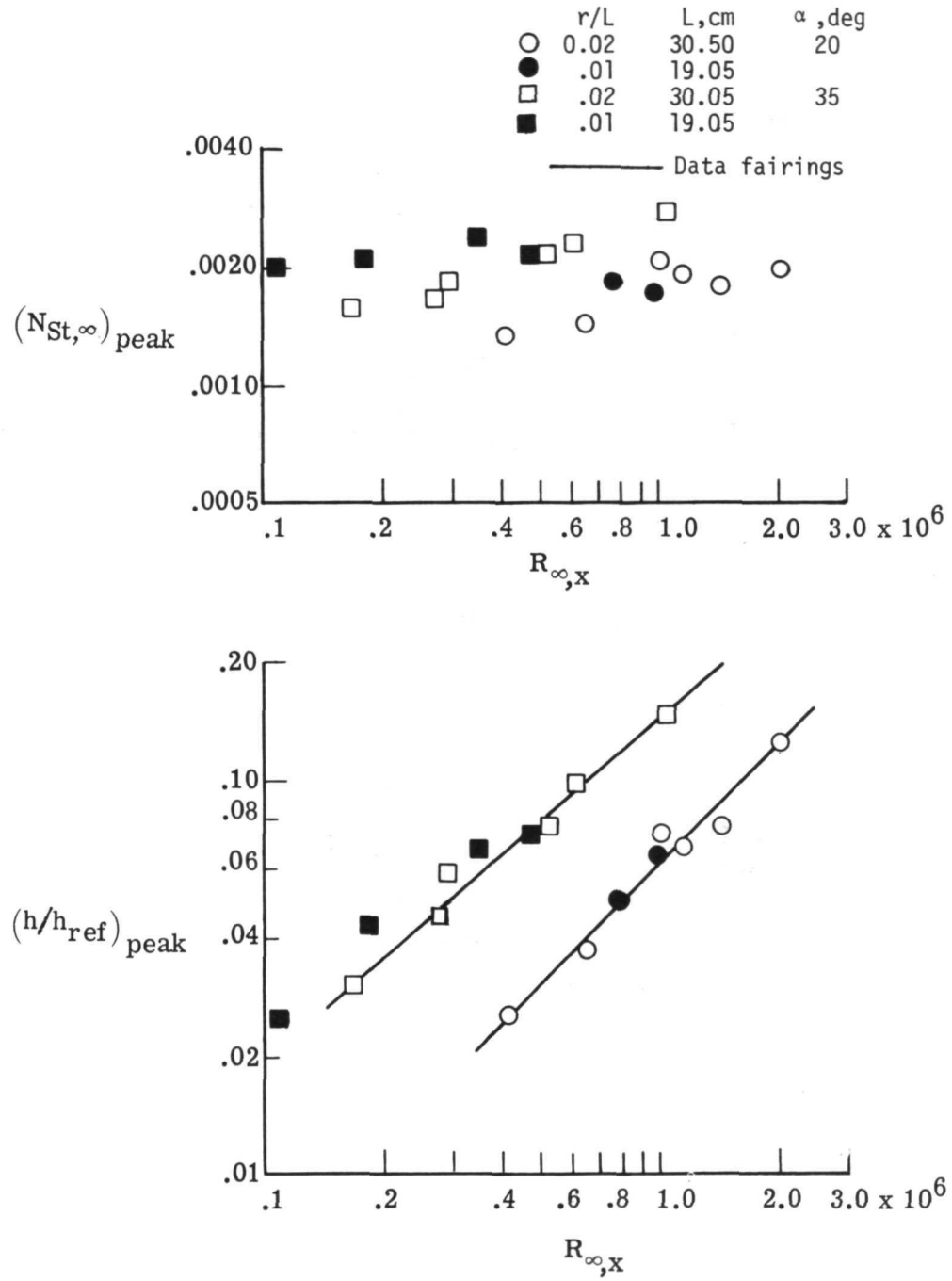

Figure 15.- Correlation of vortex-induced peak heating with Reynolds number based on distance to peak heating. $M_\infty = 6$; delta-wing orbiter.

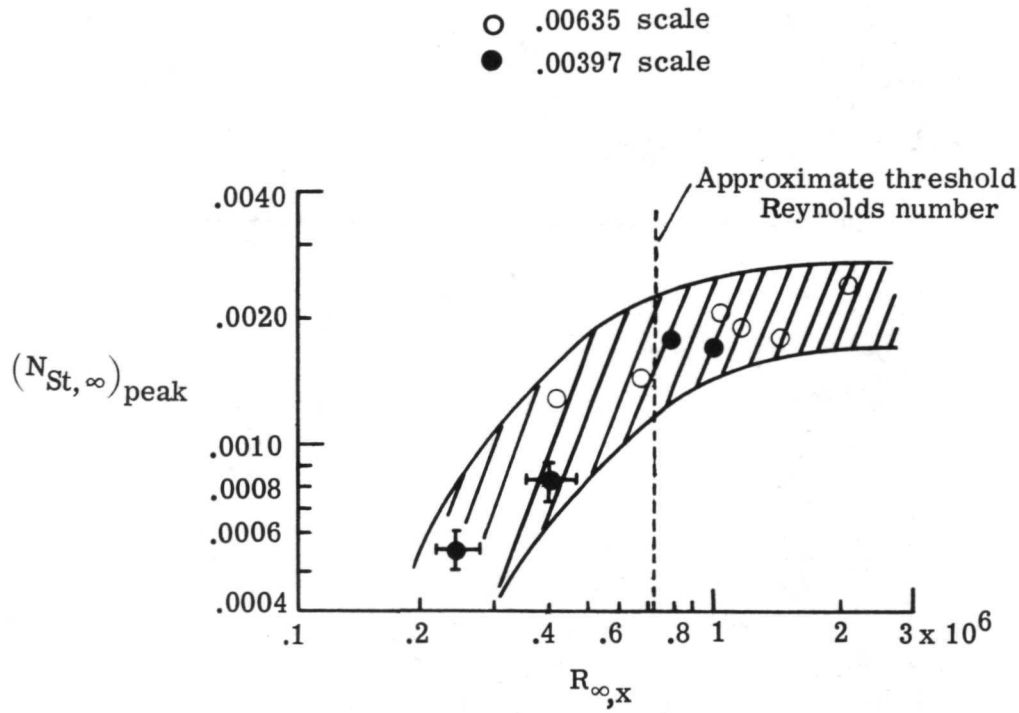

Figure 16.- Threshold Reynolds number for delta-wing orbiter.
$M_\infty = 6$; $\alpha = 20^o$.

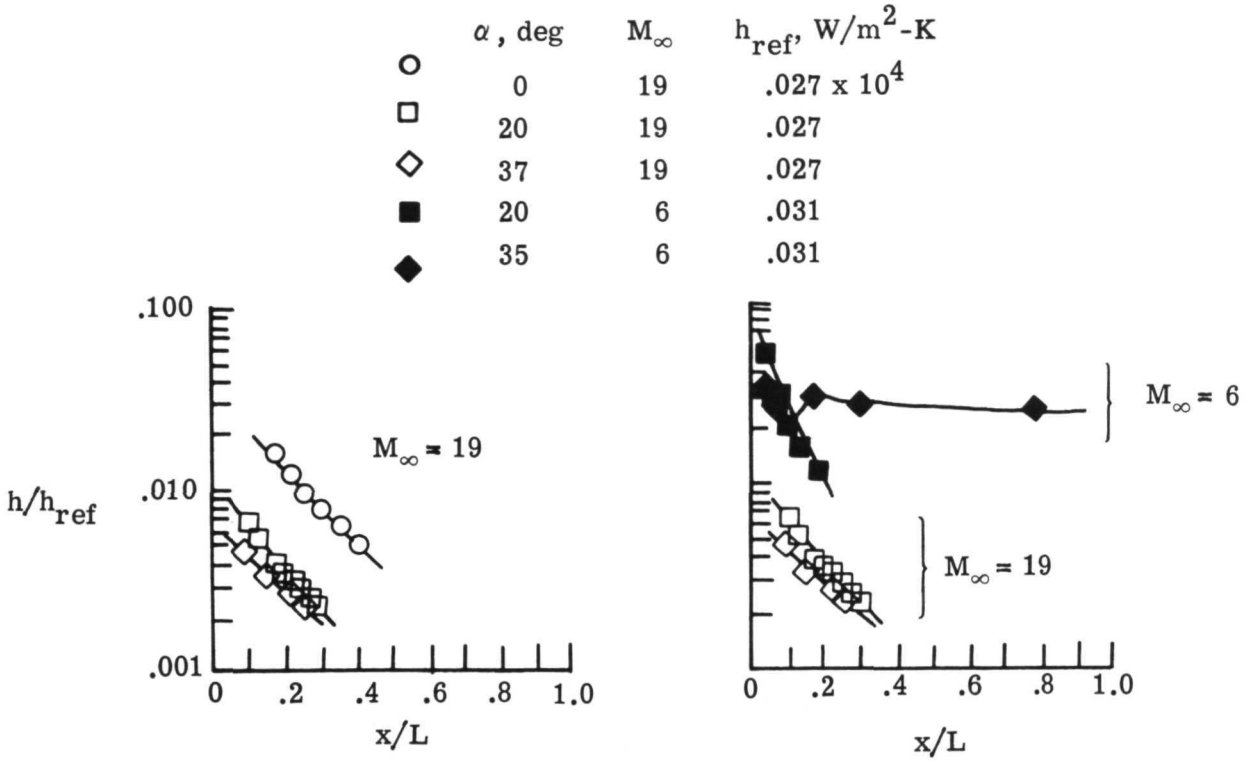

Figure 17.- Lee-surface heating at various Mach numbers. $R_{\infty,L} \approx 0.7 \times 10^6$; 0.00397-scale delta-wing orbiter.

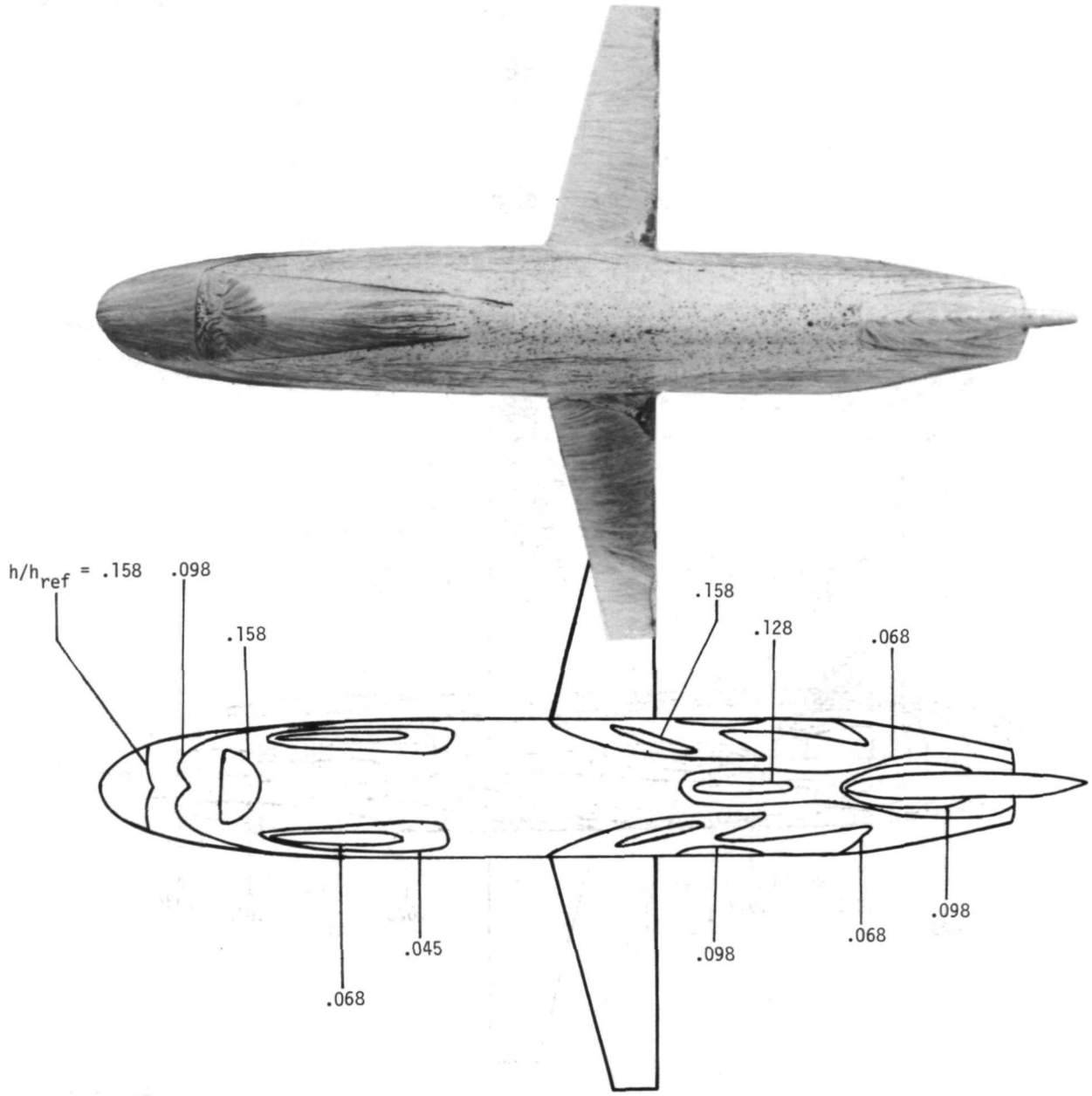

(a) $\alpha = 0^{o}$.

Figure 18.- Surface flow and heating on 0.00725-scale straight-wing orbiter. $M_{\infty} = 6$; $R_{\infty,L} = 4.3 \times 10^{6}$.

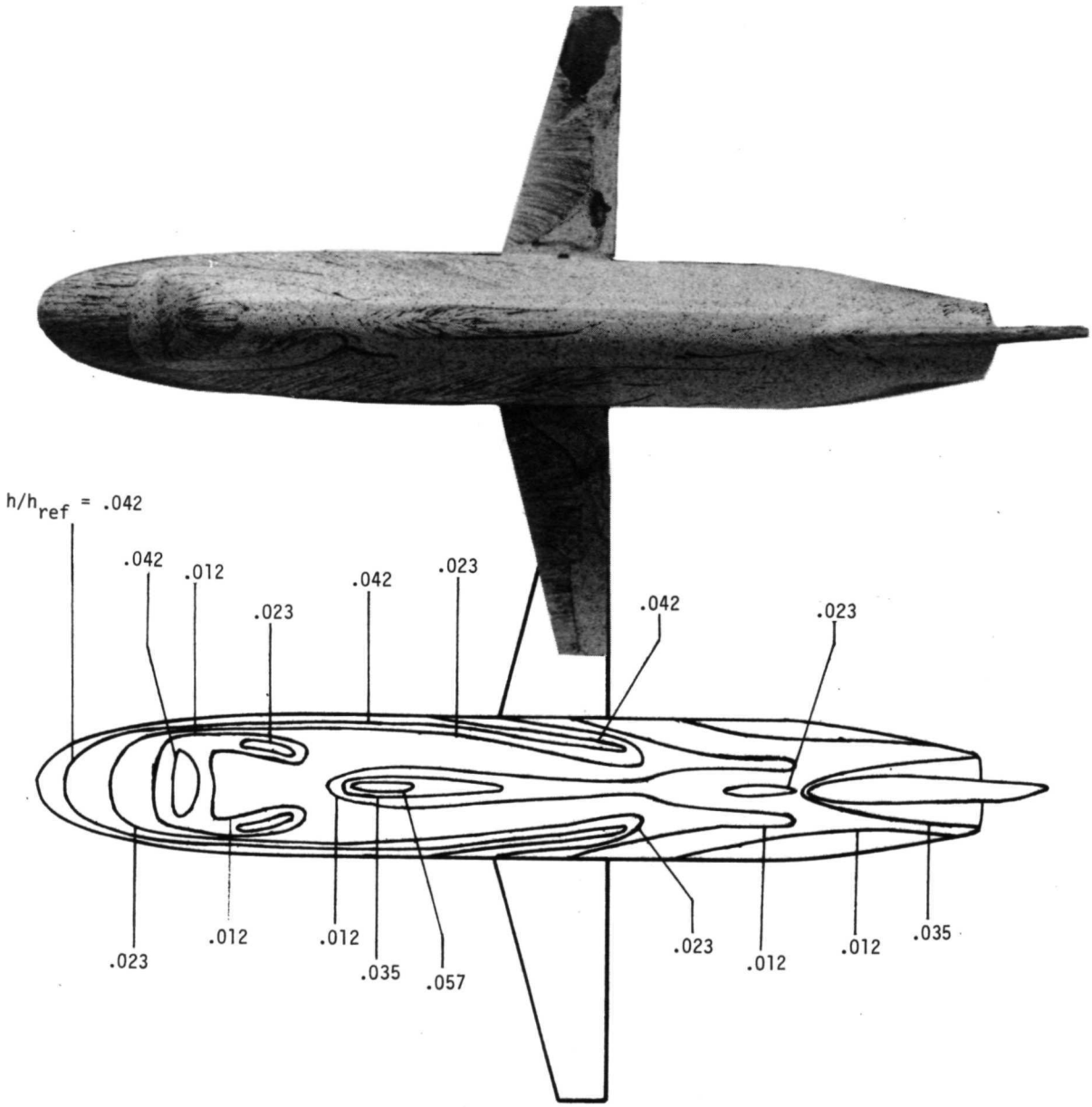

L-72-6547

(b) $\alpha = 20^{o}$.

Figure 18.- Continued.

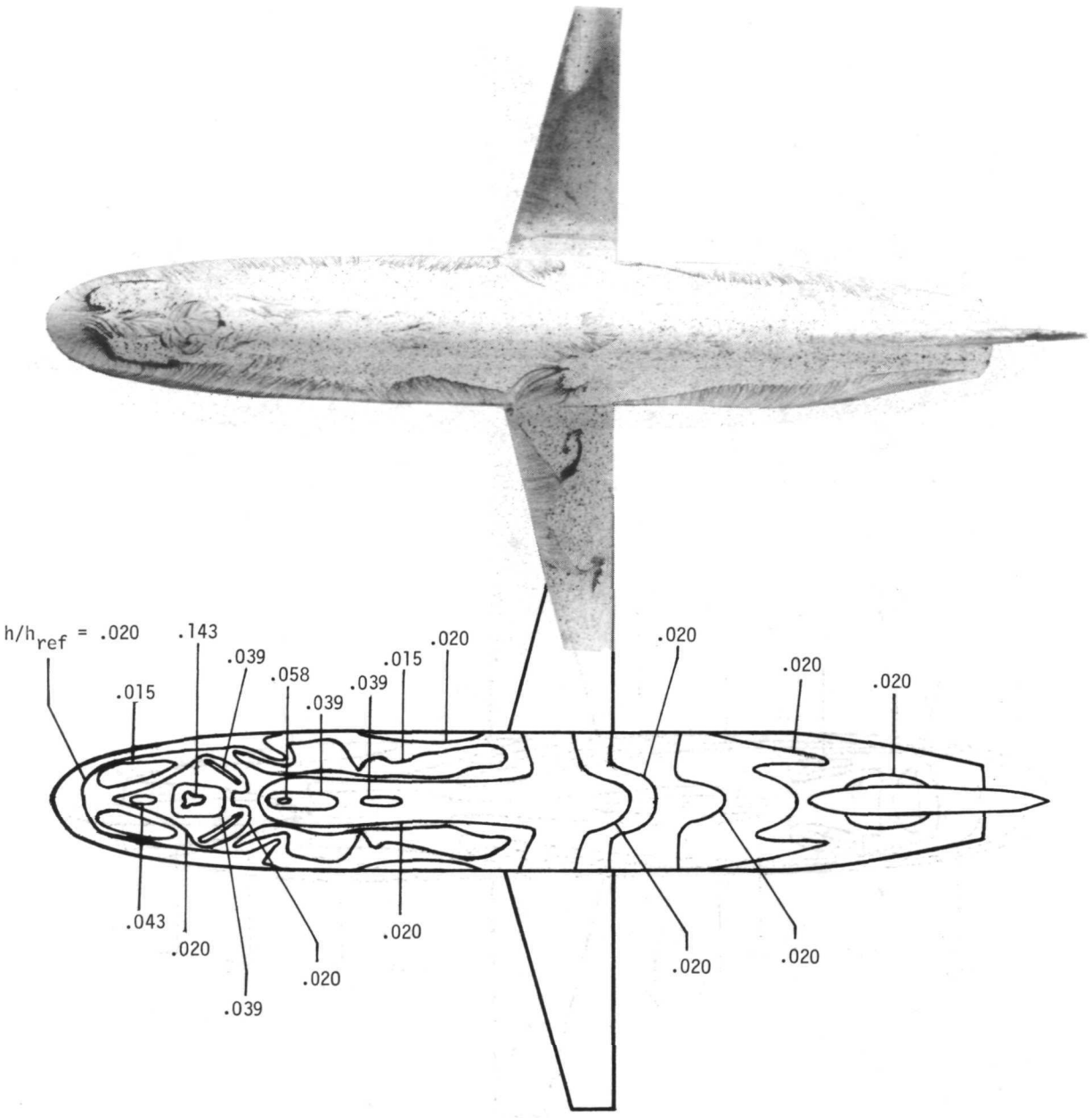

L-72-6548

(c) $\alpha = 50^{o}$.

Figure 18.- Concluded.

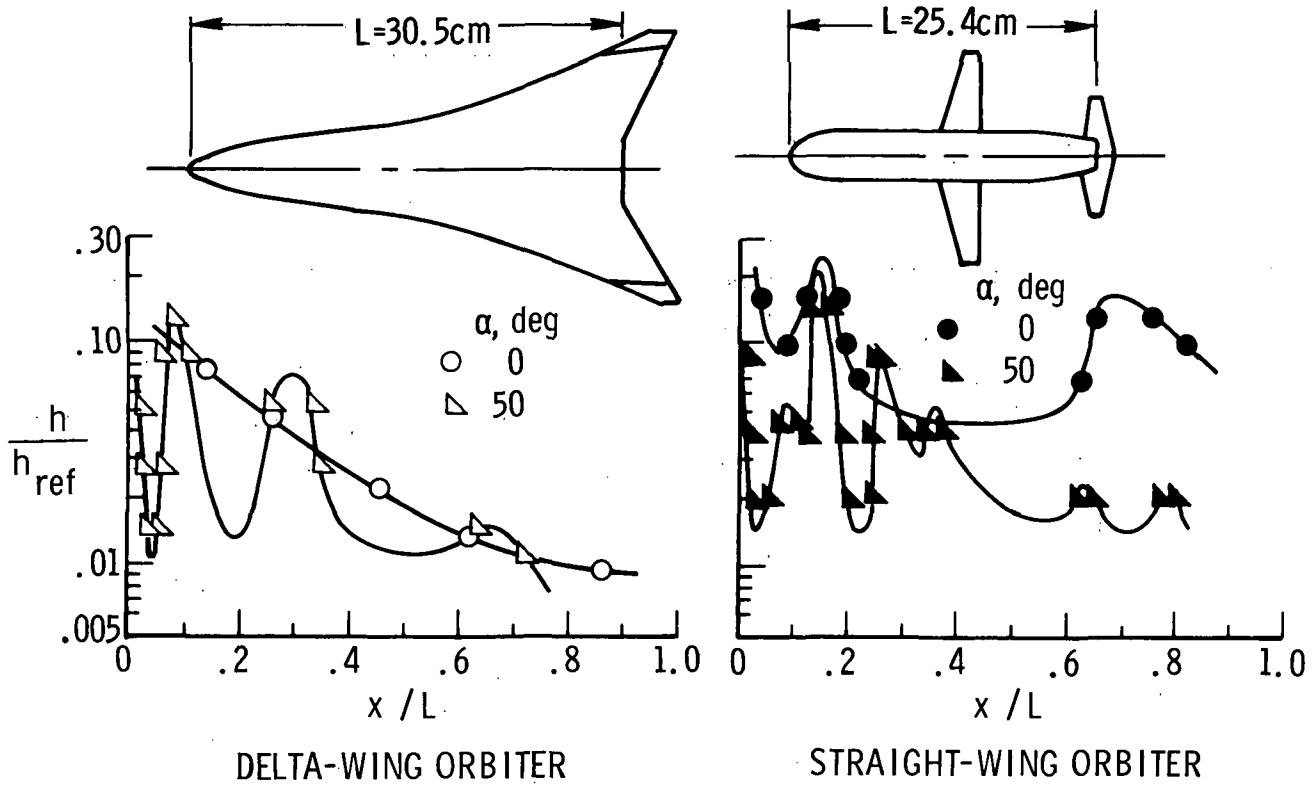

Figure 19.- Heating on lee meridian of delta-wing and straight-wing orbiters. $M_\infty = 6$; $R_\infty = 1.7 \times 10^7$ per meter.

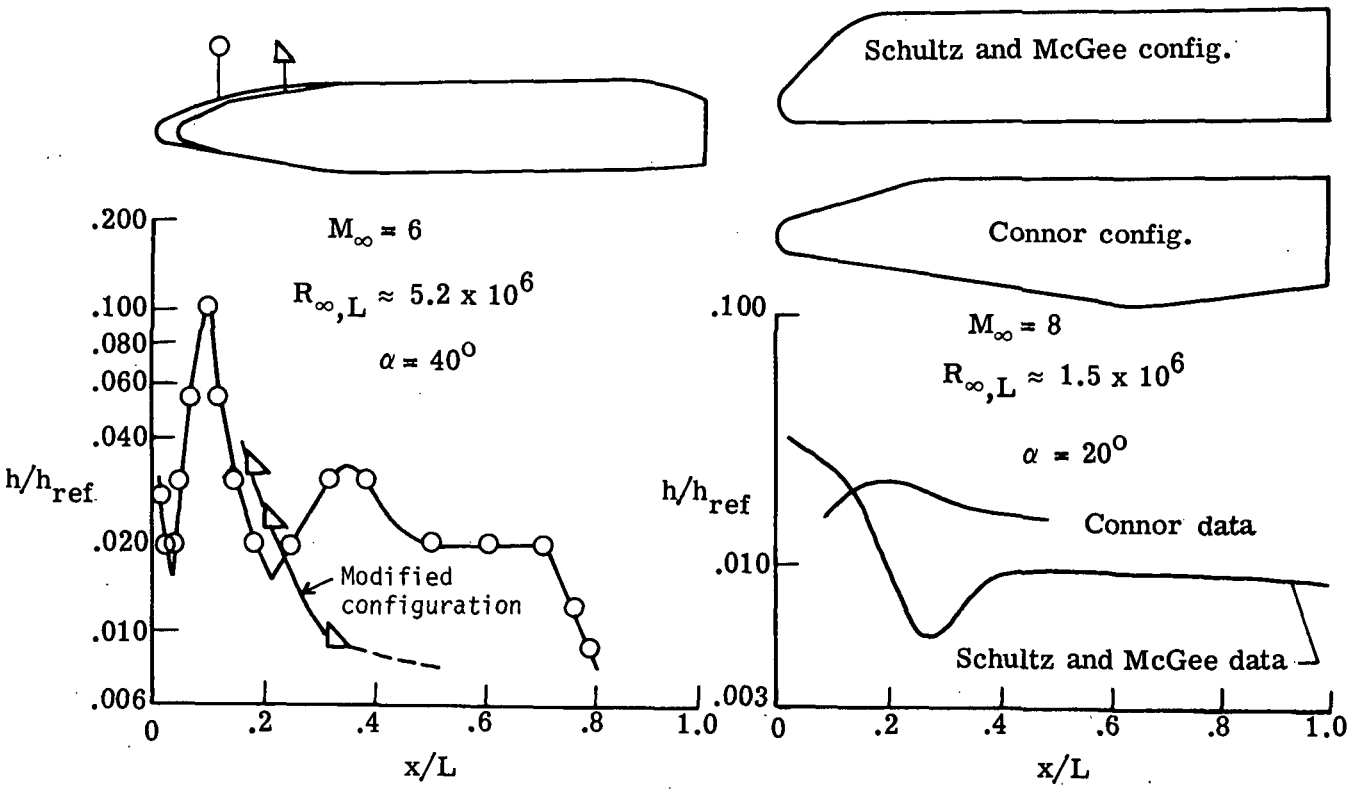

Figure 20.- Effect of lee-surface geometry on heating.

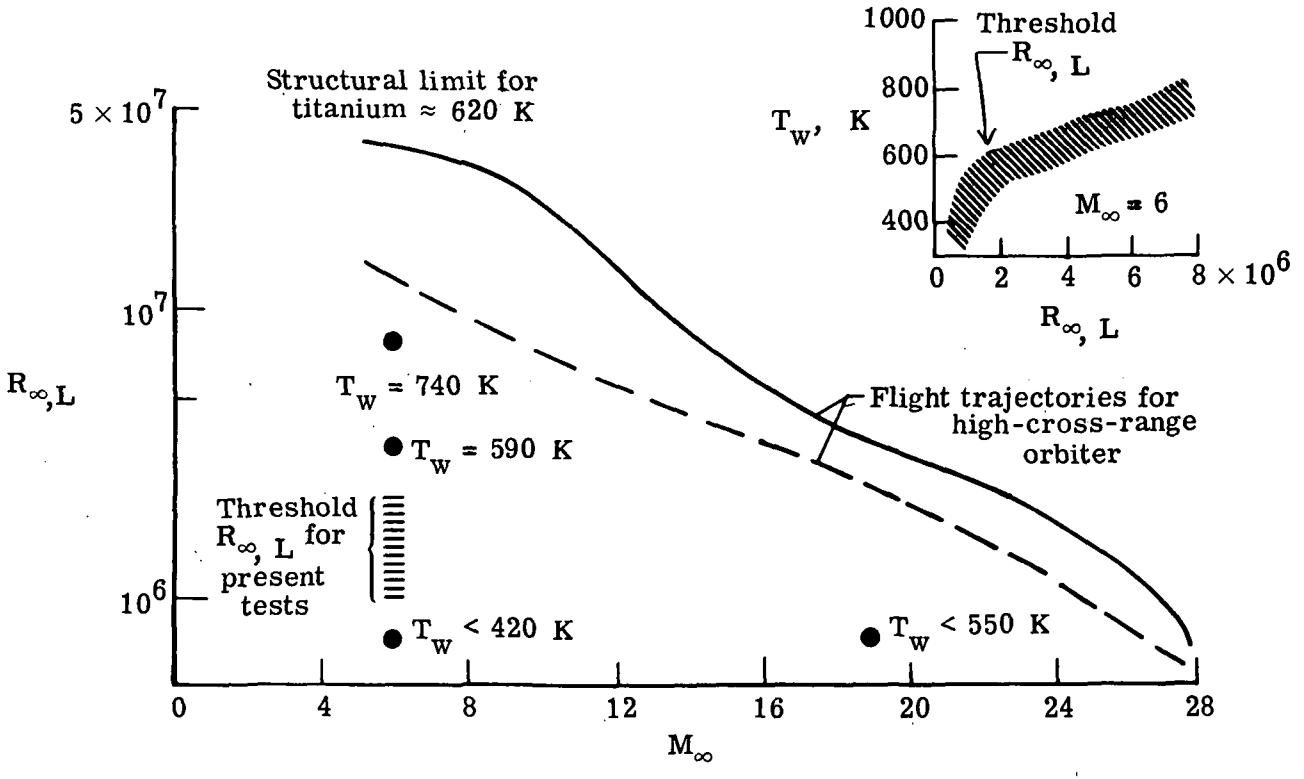

Figure 21.- Application of wind-tunnel results to flight environments. 0.00397-scale delta-wing orbiter.

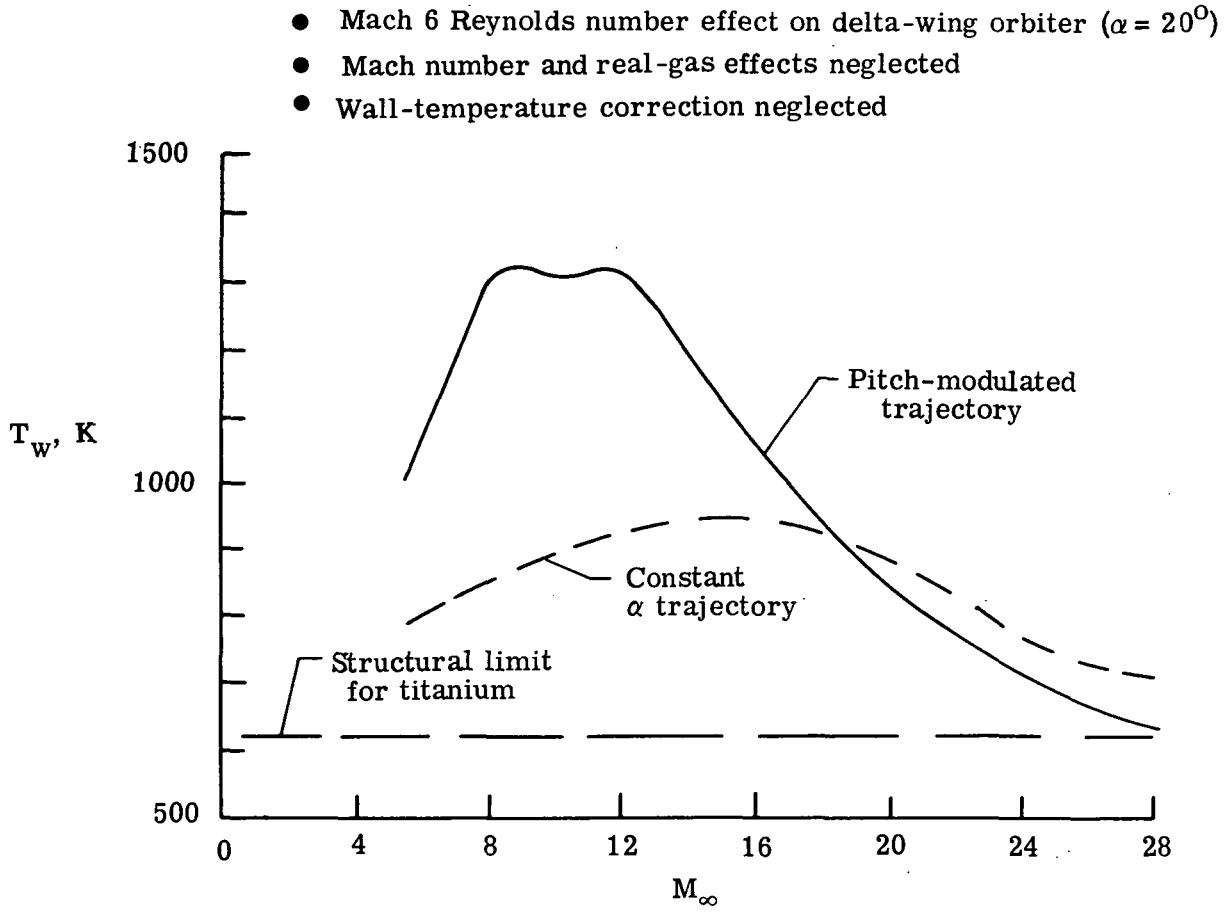

Figure 22.- Vortex-induced surface temperatures for flight.

NASA-Langley, 1972 —— 12 L-8580

NATIONAL AERONAUTICS AND SPACE ADMINISTRATION
WASHINGTON, D.C. 20546

OFFICIAL BUSINESS
PENALTY FOR PRIVATE USE $300

SPECIAL FOURTH-CLASS RATE
BOOK

POSTAGE AND FEES PAID
NATIONAL AERONAUTICS AND
SPACE ADMINISTRATION
451

U.S.MAIL

POSTMASTER : If Undeliverable (Section 158 Postal Manual) Do Not Return

"The aeronautical and space activities of the United States shall be conducted so as to contribute . . . to the expansion of human knowledge of phenomena in the atmosphere and space. The Administration shall provide for the widest practicable and appropriate dissemination of information concerning its activities and the results thereof."

—NATIONAL AERONAUTICS AND SPACE ACT OF 1958

NASA SCIENTIFIC AND TECHNICAL PUBLICATIONS

TECHNICAL REPORTS: Scientific and technical information considered important, complete, and a lasting contribution to existing knowledge.

TECHNICAL NOTES: Information less broad in scope but nevertheless of importance as a contribution to existing knowledge.

TECHNICAL MEMORANDUMS: Information receiving limited distribution because of preliminary data, security classification, or other reasons. Also includes conference proceedings with either limited or unlimited distribution.

CONTRACTOR REPORTS: Scientific and technical information generated under a NASA contract or grant and considered an important contribution to existing knowledge.

TECHNICAL TRANSLATIONS: Information published in a foreign language considered to merit NASA distribution in English.

SPECIAL PUBLICATIONS: Information derived from or of value to NASA activities. Publications include final reports of major projects, monographs, data compilations, handbooks, sourcebooks, and special bibliographies.

TECHNOLOGY UTILIZATION PUBLICATIONS: Information on technology used by NASA that may be of particular interest in commercial and other non-aerospace applications. Publications include Tech Briefs, Technology Utilization Reports and Technology Surveys.

Details on the availability of these publications may be obtained from:

SCIENTIFIC AND TECHNICAL INFORMATION OFFICE

NATIONAL AERONAUTICS AND SPACE ADMINISTRATION

Washington, D.C. 20546